AGU ADVANCING EARTH AND SPACE SCIENCE

Key Points:
- Extensive methane bubble plumes have been discovered on the Puget Sound seafloor
- The emission sites of these plumes are associated with major fault zones that penetrate the Cascadia forearc
- Dissolved methane arising from the plumes is mixed throughout the estuary by tides and local mixing

Author Contributions:

Formal analysis: Susan L. Hautala, Tamara Baumberger, Sharon L. Walker, Junzhe Liu, Nicholas D. Ward, Chenyu Wang
Investigation: H. Paul Johnson, Tor A. Bjorklund, Sharon L. Walker, Chenyu Wang
Methodology: H. Paul Johnson, Susan G. Merle, Tor A. Bjorklund, Susan L. Hautala, Tamara Baumberger, Junzhe Liu, Nicholas D. Ward, Chenyu Wang
Resources: H. Paul Johnson, Tor A. Bjorklund, Nicholas D. Ward
Software: Susan G. Merle, Susan L. Hautala

Methane Plume Emissions Associated With Puget Sound Faults in the Cascadia Forearc

H. Paul Johnson[1], Susan G. Merle[2], Tor A. Bjorklund[1], Susan L. Hautala[1], Tamara Baumberger[2], Sharon L. Walker[3], Junzhe Liu[1], Nicholas D. Ward[1,4], and Chenyu Wang[1]

[1]School of Oceanography, University of Washington, Seattle, WA, USA, [2]Cooperative Institute for Marine Resources Studies – Oregon State University, and NOAA PMEL Earth Ocean Interactions Program, Newport, OR, USA, [3]NOAA/Pacific Marine Environmental Lab, Seattle, WA, USA, [4]Coastal Sciences Division, Pacific Northwest National Laboratory, Sequim, WA, USA

Abstract Methane gas plumes have been discovered to issue from the seafloor in the Puget Sound estuary. These gas emission sites are co-located over traces of three major fault zones that fracture the entire forearc crust of the Cascadia Subduction Zone. Multibeam and single-beam sonar data from cruises conducted in years 2011, 2018, 2019, 2020, and 2021 identified the acoustic signature of 349 individual bubble plumes. Dissolved CH_4 gas from the plumes combines to elevate seawater methane concentrations of the entire Puget Sound estuary. Fluid samples from adjacent terrestrial hot springs and deep-water wells surrounding the estuary contain a helium-3 isotope signature, suggesting a deep fluid source located near the underlying Cascadia Subduction Zone plate interface. However, limited data from this pilot study suggest that Puget Sound seawater emission sites lack both similar chemical isotope signatures and elevated thermal anomalies that would be expected from association with a deep plate-interface reservoir. A shallow reservoir within the Holocene sediments that cover the older Puget Sound basement with horizontal transfer to the thinly covered Alki Point and Kingston Arch anticlines is also a possibility, as has been suggested for other methane seep areas. The existence of vigorous marine methane plumes arising from areas of thin sediment cover associated with deeply penetrating forearc fault zones but presenting no thermal or chemical anomalies found in other similar forearc environments, remains an unresolved paradox.

Plain Language Summary Puget Sound is a large inland sea located in western Washington State where seawater circulation is dominated by vigorous tidal forcing from the North Pacific Ocean. The deep Puget Sound is the largest estuary in North America measured by contained water volume and the second largest estuary after Chesapeake Bay in terms of area. Shipboard sonar images have revealed approximately 349 bubble plumes of methane gas and fluid rising from the seafloor of the estuary. Large clusters of bubble plume sites are concentrated over the major regional fault zones that penetrate the western North American plate beneath Puget Sound, including the South Whidbey Island Fault, the Seattle Fault, and the Tacoma Fault Zones. Although the forearc Puget Basin is surrounded by terrestrial hot springs and water wells that show a clear chemical isotope signature of fluid arising from the underlying Cascadia Subduction Zone plate interface, based on our limited sampling there is currently no evidence for similar chemical or temperature anomalies in the Puget Sound plumes and the source of the methane bubble plumes is still unidentified.

1. Introduction

Natural marine seeps of methane are a small but still important source of a strong greenhouse gas that enters the global environment. Methane emissions from the surface waters of estuaries into the atmosphere arise from a multitude of sources including rivers, benthic production, and simple diffusion from organic-rich sediments and these are poorly constrained on a global scale (Rosentreter et al., 2021).

Active methane emissions from coastal margins have been known for over 50 years (Hovland & Judd, 1992 and references therein). Present day methane emission estimates, compiled with large uncertainties, indicate that between 3 and 48 Tg/y of methane is released to the atmosphere from marine seeps, including sources that are both thermogenic and biogenic in origin (Etiope, 2012; Hornafius et al., 1999; Razaz et al., 2020). Globally, the largest known concentrations of marine methane emission sites are on active continental margins that overlie subduction

Writing – original draft: H. Paul
Johnson, Susan G. Merle, Tor A.
Bjorklund, Susan L. Hautala
Writing – review & editing: Susan L.
Hautala, Tamara Baumberger, Sharon L.
Walker, Nicholas D. Ward, Chenyu Wang

zones, and the Cascadia margin beneath is an unusually well-studied example (Baumberger, et al., 2018; Embley et al., 2017; Hautala et al., 2014; H. P. Johnson et al., 2019; Merle et al., 2021; Riedel et al., 2018; Salmi et al., 2011). Gas emissions are also identified in abundance on some passive coastal margins, although the mechanism for producing those methane seeps appears to differ from those present on subduction zone margins (Garcia-Tigreros et al., 2020; Mau et al., 2012, 2015; Plaza-Faverola & Keiding, 2019; Ruppel & Kessler, 2017; Skarke et al., 2014).

Multibeam and single-beam sonar data from recent cruises revealed extensive bubble plume fields present within the Puget Sound and Hood Canal estuaries. Sonar data from 18 cruises using two different data acquisition systems contributed to the plume identifications. In 2011, the RV Thompson returned to its Seattle home port at the end of cruise TN265. Atypically, the EM302 multibeam sonar was left in the data acquisition mode during transit through northern Puget Sound, and included sonar return data from acoustic reflectors within the water column. These data were archived in the Rolling-Deck-2-Repository database.

The archived RV Thompson multibeam water column data in Puget Sound were processed for on-going compilations of coastal methane emission sites on the outer Cascadia Margin and an unanticipated North-South oriented field of gas bubble plumes was discovered along the axis of the uplifted Kingston Arch anticline in northern Puget Sound (Figure 1; Pratt et al., 1997). This new emission field was located where the edge of approximately NW-SE trending South Whidbey Island Fault (SWIF; S. Y. Johnson et al., 1996; Sherrod et al., 2008) intersects a roughly North-South trending fault imaged by S. Y. Johnson et al. (1999) (Figure 1). The Kingston Arch has been described as a gentle anticline that forms the northern boundary of the Seattle Basin and has been topographically incised by Puget Sound but does not appear to be bounded by any previously mapped faults (Pratt et al., 1997; S. Y. Johnson et al., 1994, 1996).

Following the 2011 RV Thompson cruise, an additional 17 cruises on the *RV Carson* were conducted in 2018, 2019, 2020, and 2021, with most of these cruises following tracklines determined by other academic class and research objectives rather than searching for active bubble plume sites. Gas bubble plumes were identified in the sonar records from the 38 kHz single-beam Simrad ES38B with post-cruise data processing with the ESP3 program (Ladroit et al., 2020; Veloso et al., 2015). These cruise sonar records provided additional evidence of gas bubble plumes that are widely distributed throughout the water columns of Puget Sound, Hood Canal and even extend into Lake Washington (Figure 1).

The plume site locations appear to be stable in time, although repeat sonar imaging only exists for cruises TN265, RC0014, RC0019, RC0022, RC0038, RC0047a, and RC0052. These repeat cruises show that plume sites can be re-identified at different times using slightly different sonar frequencies, including both 30 kHz multibeam sonar on the RV Thompson and 38 kHz single beam sonar on the RV Carson, and that emissions have remained active for at least the last 10 years. Although single isolated bubble plumes were found distributed throughout the estuary, the primary clusters of bubble streams are concentrated above three major fault zones (Figure 1).

Acoustic reflections in the sonar data indicate that a small portion of the gas bubbles plumes reach from the seafloor to the sea surface within the plume fields located at both Kingston Arch and the Alki Uplift, which have water depths of 180 and 160 m, respectively (Figures 2–5). The acoustic observations of bubbles reaching the surface were confirmed by science party observations on the RV Carson deck that identified gas bubbles breaking the water surface at both sites. The presence of a frothy film on the water surface directly overlying the immediate area of the sites but absent from the adjacent waters was also observed, similar to observations at other methane emission regions. This suggests that the bubbles are likely organically coated, a phenomenon that impacts both bubble rise velocity and can slow methane gas diffusion into the water column (Fu et al., 2020; Leifer, 2010; Leifer & MacDonald, 2003; Leifer & Patro, 2002). The success of quasi-random tracklines of the RV CARSON in identifying the plumes, with a limited sonar seafloor acoustic footprint of approximately 25-m diameter at 200-m water depth, implies there are still many unidentified plumes within the estuary that are not included in the present inventory.

In this study, we present the identification of 349 Puget Sound gas bubble plumes using single-beam sonar and traditional Niskin bottle sampling. We then describe the inconsistency presented by our observed normal seawater emission chemistry and temperature data that is in contrast to the site locations being positively correlated to the deeply penetrating fault zone traces in the Cascadia forearc. The sub-surface reservoir for the plume gas/fluid is not resolved or explained by our limited pilot-study data, and we present potential alternative hypotheses for
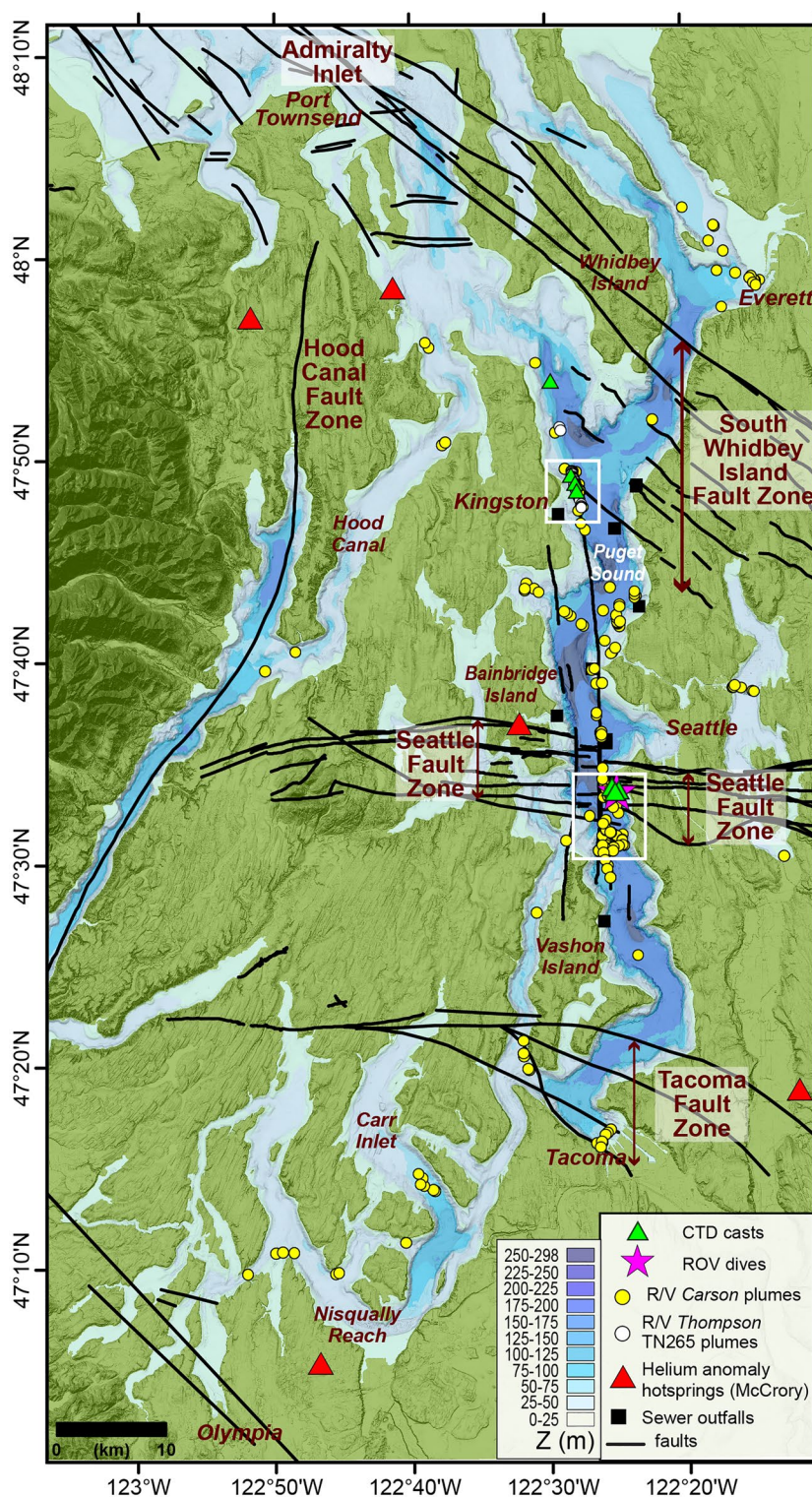
Figure 1. Map of Puget Sound and Hood Canal in north-central Washington State. Yellow circles are sites of individual bubble plume emissions based on CARSON single-beam 38 kHz sonar. Black lines are trace projections of the South Whidbey Island Fault, Seattle Fault Zone, and Tacoma Fault Zone faults and the N-S Hood Canal and Puget Sound faults of S. Y. Johnson et al. (1999). Black squares are urban sewer outfalls. Red triangles are locations of hot springs and water wells with helium isotope anomalies indicative of a deep subduction zone source (McCrory et al., 2016). Green triangles are CTD casts from the CARSON. Fault traces are from the USGS Active Faults Database, updated from Angster et al. (2020), https://doi.org/10.5066/P9X2RR2T, and amalgamated with S. Y. Johnson et al. (1999).
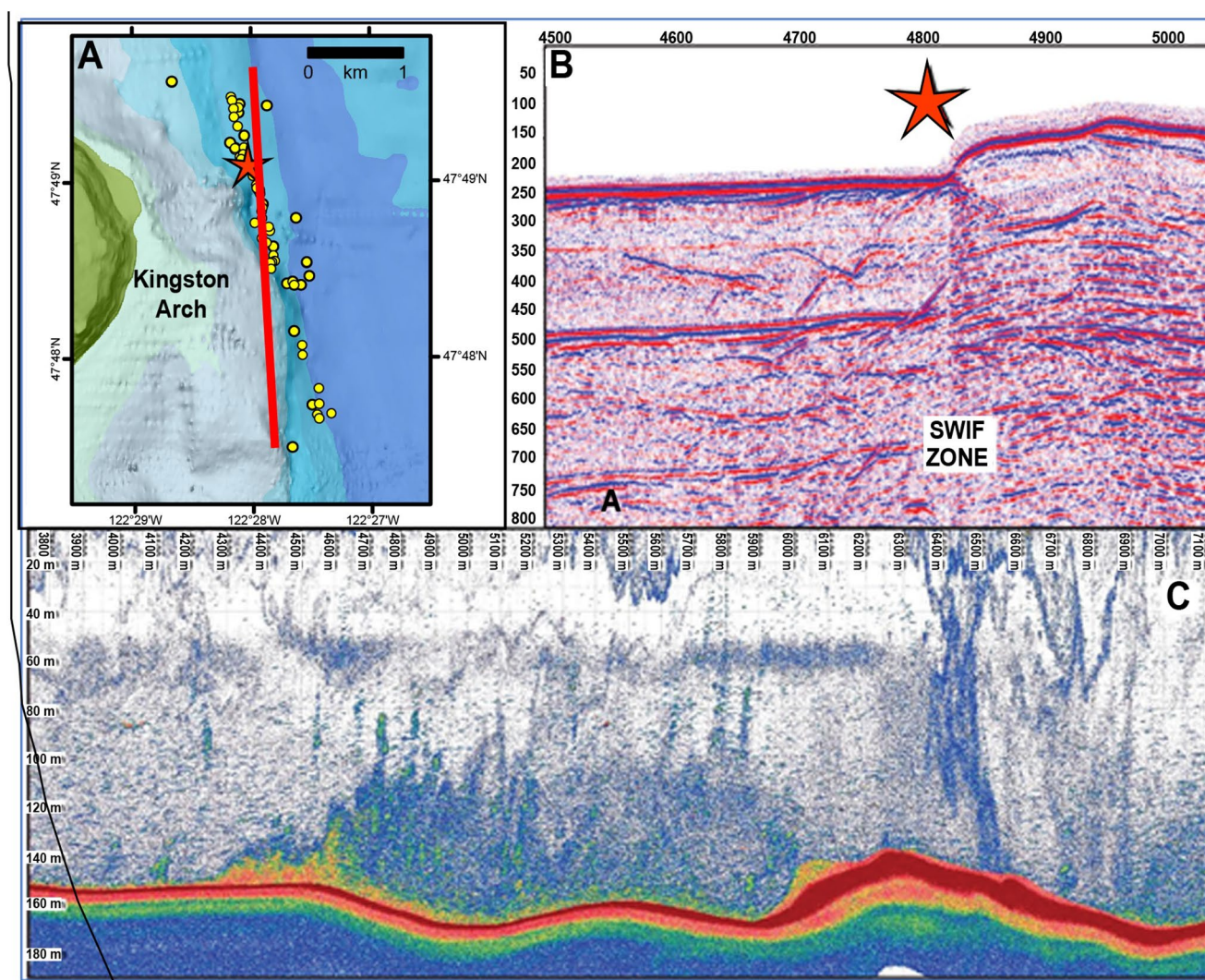
Figure 2. (a) Yellow circles show bubble plume locations from CARSON sonar acquired near Kingston Arch with red star indicating location of fault offset co-located in panel (b). Red line is MCS trackline for image in panel (b). (b) Offset sediment layers from the South Whidbey Island Fault Zone from archived MCS data (S. Y. Johnson et al., 1996). Red stars in panels (a and b) are co-located. Vertical exaggeration is 2.5:1. (c) CARSON 38 kHz sonar image of bubble plumes at Kingston Arch, showing both gas bubbles (center) and fluid emissions (right) at position of red star in panel (a). Heavy red trace is the bottom reflection.

the source of these abundant plumes. We also discuss potential future methods for resolving whether these fault zones are direct fluid pathways from a deep reservoir of thermogenic CH_4 via the forearc fault zones or if instead the methane gas is biogenically derived from organic material present within recently deposited sediments.

2. Methods

2.1. Separating Anthropogenic and Geological Sources

Understanding the source region of bubble plumes occurring within any urban estuary first requires separation of geological emissions from anthropogenic gas bubbles from sewer outfalls, storm drains and recent and historical dredge deposits. Storm drains in Puget Sound are clearly noted in NOAA navigational charts, are located near the shoreline in shallow water depths (<20 m), and their freshwater discharge is unlikely to produce gas bubbles from the seafloor. Urban sewer outfalls are located in deeper water and their freshwater discharge can produce temporary gas plumes which are well-mapped (Figure 1). For example, a weak column of gas issuing from the Seattle West Point sewer outfall was observed during one *RV CARSON* cruise and was excluded from the plume inventory.
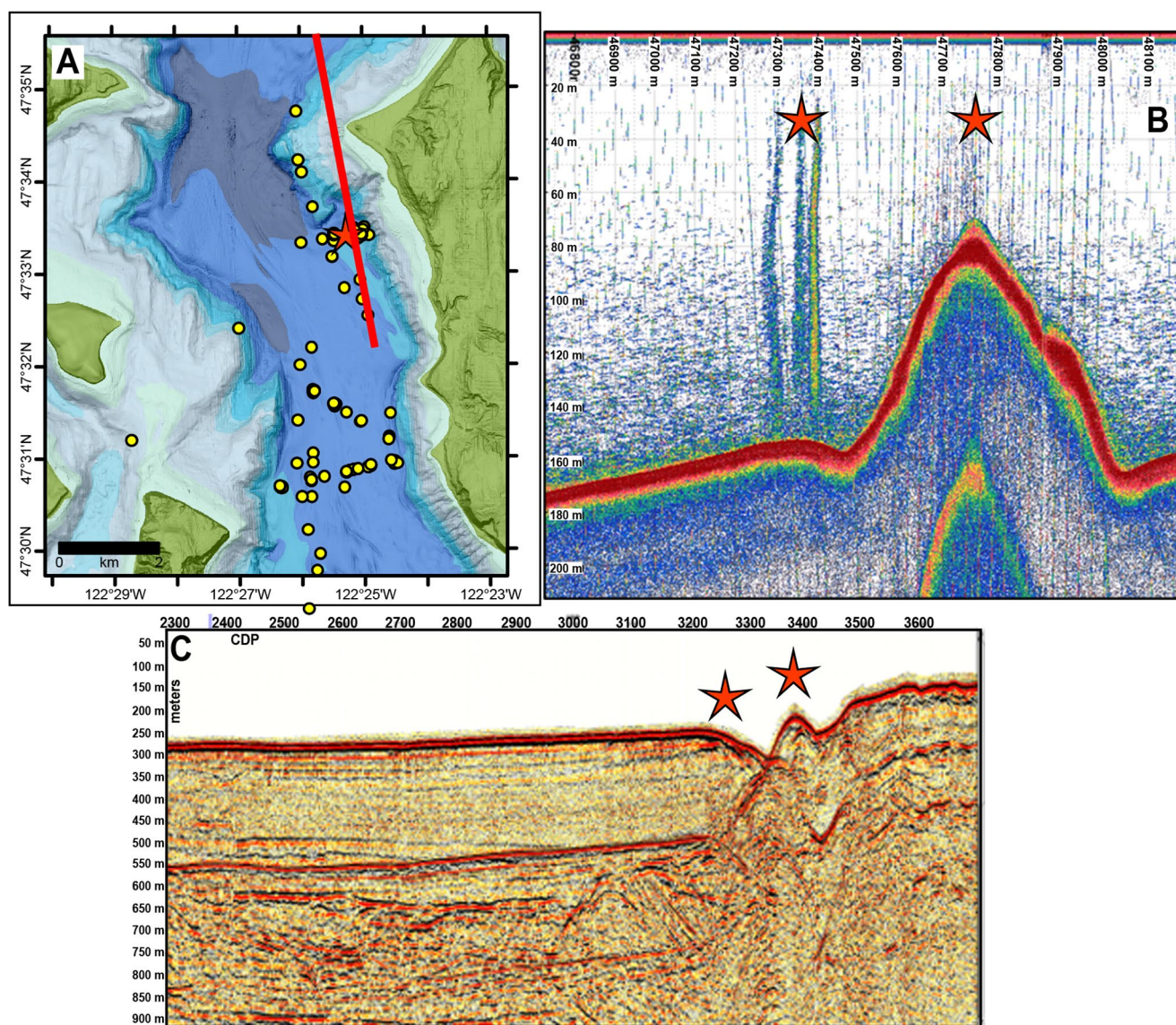
Figure 3. (a) Yellow circles are bubble plume locations near Alki Point within the projections of the Seattle Fault Zone (Figure 1). Red line is approximate trackline for MCS image in panel (b). Red stars in all three panels are co-located. (b) CARSON sonar image of gas plumes shown in panel (a). (c) Archive MCS profile of sub-surface structures beneath the bubble plume site, showing basement rock uplift. Data from S. Y. Johnson et al. (1999). VE = 2.9:1.

Dredge dump sites that were previously legally permitted are also well-mapped although these dumps have been tightly restricted in Puget Sound over the last several decades. Mud slides and land-fill dumps from early urban development can also be recognized by detailed bathymetric mapping. However, a controlled photography and coring study in the Sound indicated that over 85% of the initial volume of dredge and slump material is removed by the vigorous tidal currents within a period of less than 4 months, and complete consolidation of any residual sediment matrix material is also completed within this short time interval (Nittrouer & Sternberg, 1975). As occurs with riverine input into the estuary, these potential anthropogenic sources of methane are associated with buoyant freshwater. Previous studies have shown that methane concentrations in low salinity river water decrease due to oxidation by methanotrophic bacteria almost immediately (hours) after exposure to saline water (Boetius & Wenzhöfer, 2013; de Angelis & Lilley, 1987; Pack et al., 2015; Schubert et al., 2006; Upstill-Goddard et al., 2000).
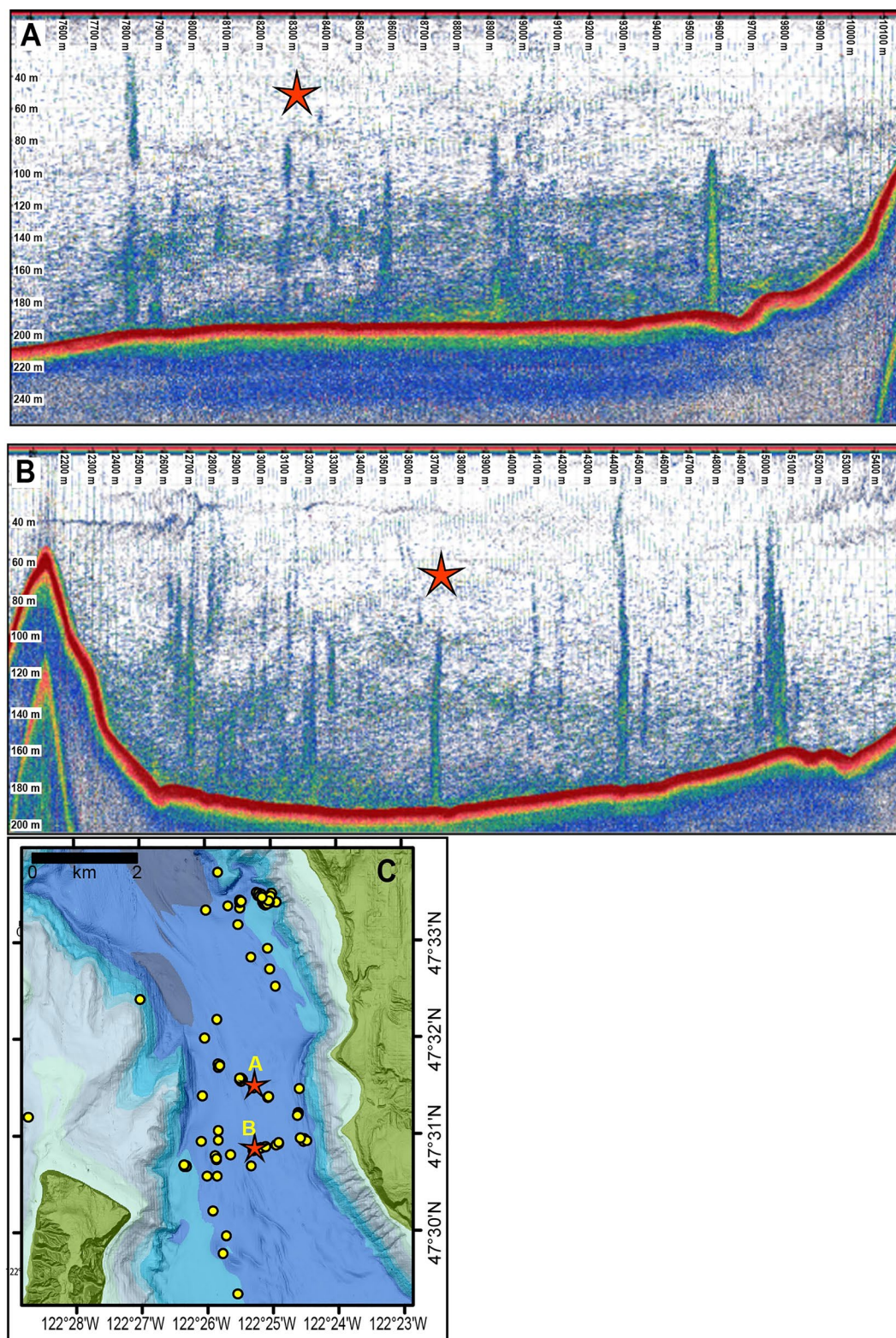
Figure 4. (a and b) RV Carson 38 kHz sonar profiles across Puget Sound over the projected locations of the Seattle Fault Zone, showing plume fields extending entirely across the Seattle basin (Figure 1). Sonar image locations are shown on lower map. (c) Map showing locations of sonar profiles in panels (a and b). Red stars are the center of the profiles in panels (a and b) shown above. Yellow circles are individual methane plume locations.
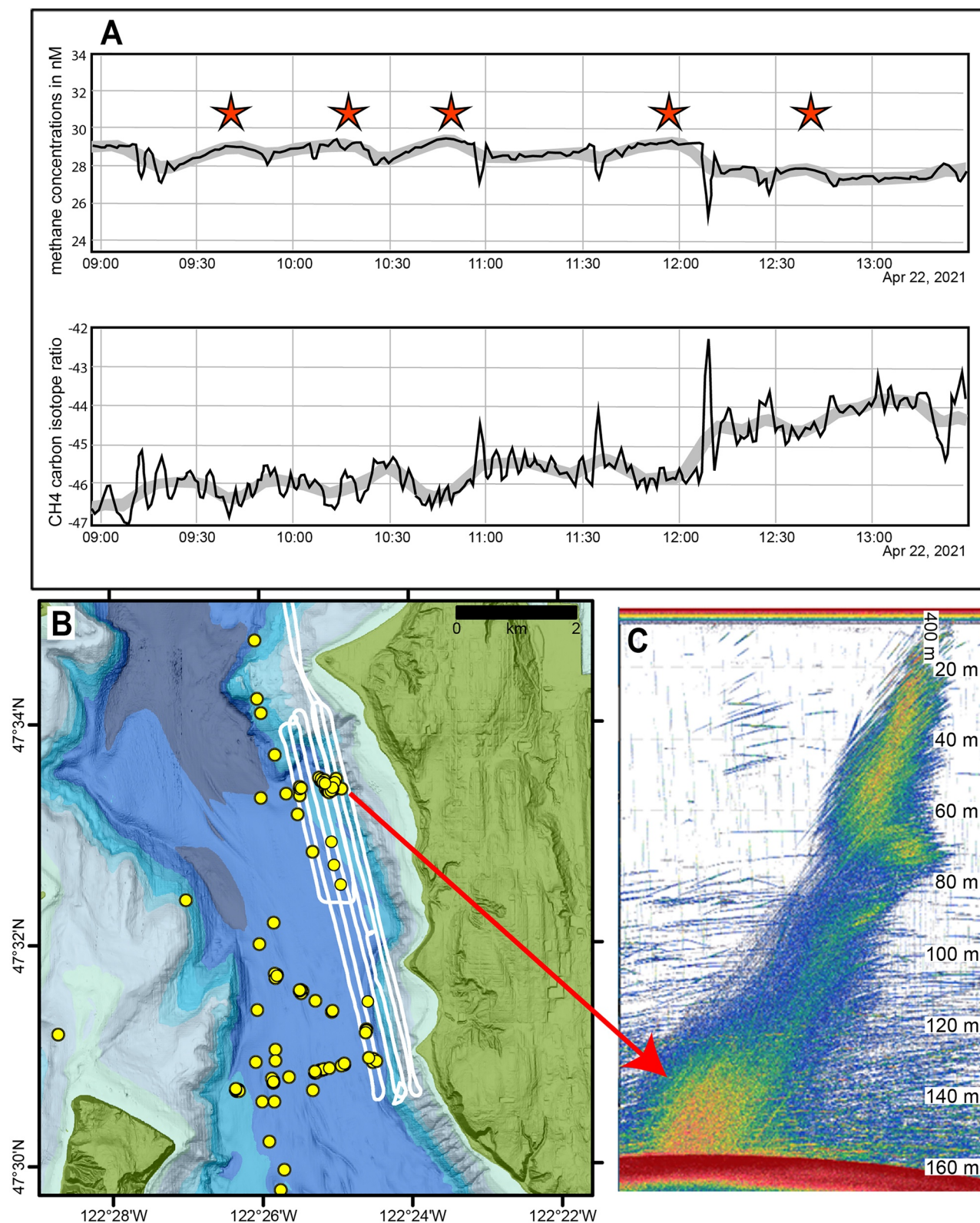
Figure 5.

2.2. Chemistry of Fluid Samples

In an attempt to determine the origin of the plume gas emissions, we sampled near-vent seawater on two short pilot cruises (RC0019 and RC0038) using Niskin bottles mounted on the RV CARSON CTD cage. The CTD employed was a Seabird 9plus. For the RC0038 cruise, Niskin bottles were also attached to a small PHANTOM 2D2HD remotely operated vehicle (ROV). Niskin bottle samples were analyzed for helium concentrations and isotopes, and the traditional seawater nutrients of silica, ammonium, and nitrate/nitrite compounds. Data from Niskin bottle samples from the Kingston plume site were also taken by CTD cast on RC0014, but only limited nutrient chemistry was done on these samples (Tables T1 and T2). On these three cruises, fluid samples obtained with Niskin Bottles on the CTD cage were obtained from within a few meters of the bubble plume orifices, as indicated by reflections from the metal cage present in the surface ship sonar images.

The three seafloor fluid samples obtained by the ROV were obtained adjacent (<1 m) to the seafloor bubble orifices using Niskin bottles mounted on the front of the ROV. However, the number of near-bottom seafloor samples was constrained by limited bottom time for the ROV, poor visibility and imprecise acoustic navigation, resulting in only three discrete fluid samples being obtained within a few 10 cm from two of the active Seattle Fault (SF)/Alki Point vent orifices (Figure 5).

2.3. Flow-Through Methane Measurements of Surface Seawater

In April 2021, a flow-through CH_4 analyzer was installed on the RV CARSON cruise RC0052 to measure surface water methane concentrations (nM) and the stable isotopic composition of methane ($\delta^{13}C$-CH_4) during a survey of the Alki Point bubble emission field (Figure 5). This analyzer was attached to the seawater intake that provided continuous flow-through surface water to the Sea-Bird thermosalinograph instrument that is part of the normal RV CARSON scientific instrumentation. Ship speed for most of the survey was 8–9 knots but slowed to 2 knots when directly over the Alki Point field (Figure 5). The partial pressure of methane (pCH_4; atmospheric units) in surface waters was measured using a headspace equilibration chamber (Frankignoulle et al., 2001) interfaced to a Los Gatos Methane Carbon Isotope Analyzer cavity ringdown spectrometer, which also provided the carbon stable isotopic data. Methane concentration range for this instrument is 10–500 ppm; precision for ^{13}C is 1 per mil, and for pCH_4 is 0.2% across the range which for 100 ppm would be ±0.2 ppm. The maximum drift for isotope measurements is 2 per mil and is not applicable for concentrations. Factory specifications and calibration data for this instrument are available in the Text S1.

Equilibration chamber headspace pCH_4 was converted to CH_4 concentrations based on the ideal gas law as follows:

$$[CH_4] = pCH_4 \times \frac{1}{R \times T} \tag{1}$$

where, R is the universal gas constant (0.082057 L atm $°K^{-1}$ mol^{-1}), and T is temperature in $°K$. The concentration of methane dissolved in the surface waters was then calculated based on the temperature-dependent Henry's Law constant (K_H) (Wiesenburg & Guinasso, 1979):

$$K_H = e^{\left[-68.8862 + \left(101.4956 \times \frac{100}{T}\right) + \left(28.7314 \, xlnln\left(\frac{T}{100}\right)\right)\right]} \tag{2}$$

where T is temperature now in $°C$ units. The delay between seawater intake and methane measurement by the shipboard analyzer is approximately 5 min.

Figure 5. CARSON survey of the Alki Point plume field with the flow-through methane analyzer sampling of the surface waters. (a) Top curve shows methane concentrations (in nM) of the surface water with red stars indicating passes over the large cluster of plume emissions. Thin black lines are unsmoothed data showing sharp turns where the seawater intake was lifted above sea level and gray curve is seven-point smoothing of the data. Bottom curve shows co-registered CH_4 carbon isotope ratio with both unsmoothed (black) and smoothed (gray) data. (b) White line of ship track for survey in panel (a), with yellow dots showing methane emission sites. (c) Image of methane bubble plume from Alki Point field from CARSON 38 kHz sonar during survey, red arrow points to plume location.
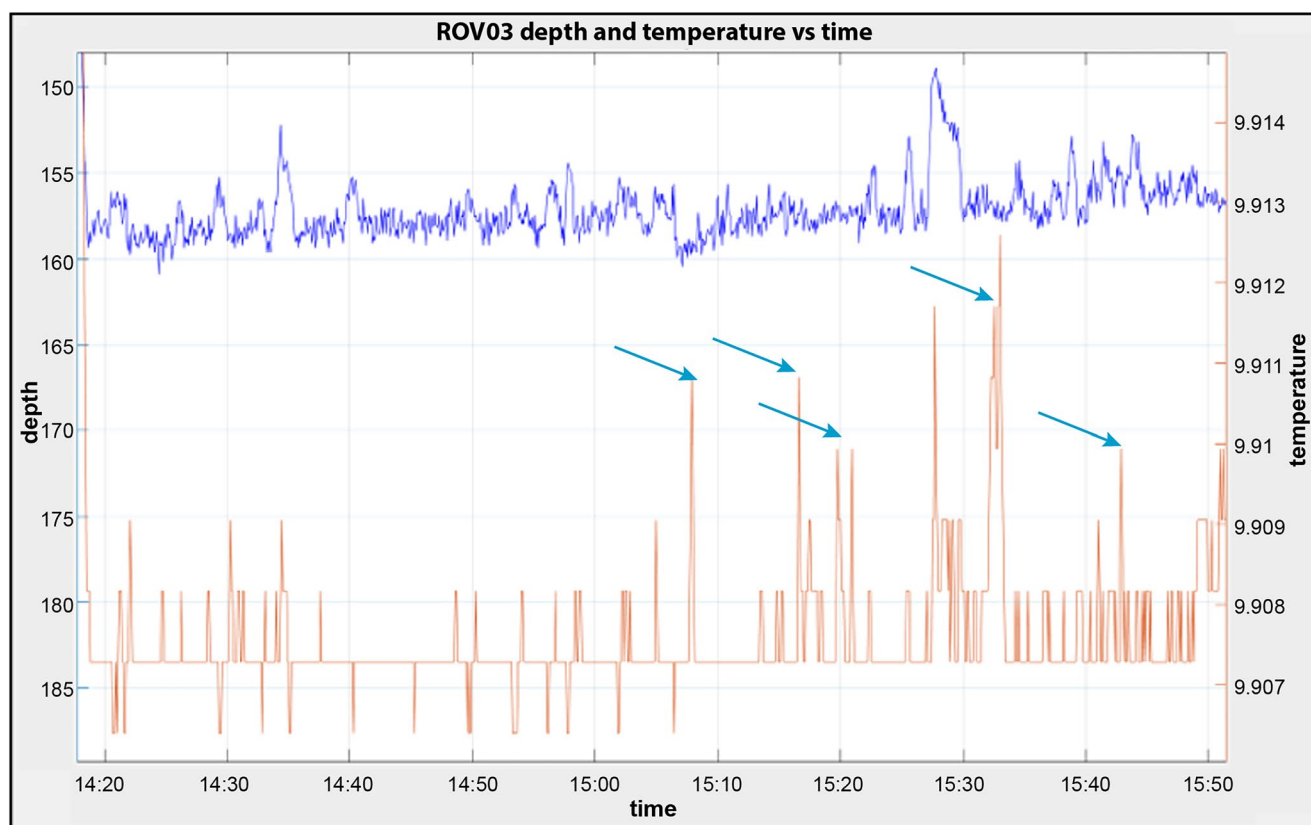
Figure 6. Top blue curve shows water depth above the bubble plume vent orifices at the Alki Point plume field, showing changes in elevation above the seafloor; shown to illustrate that the small temperature anomalies are not due to changes in altitude above seafloor. Bottom red curve shows the temperature data from the NOAA Miniature Autonomous Plume Recorder instrument. Data have abrupt changes due the sensor A2D converter resolving weak temperature variations. Arrows point to temperature anomalies associated with passage of the remotely operated vehicle directly over the vent orifices.

2.4. Helium Sampling

Samples for helium analysis were taken at the Kingston (RC0019) and Alki Point (RC0038) plume sites using standard Niskin bottles attached to the CARSON CTD cage. At the Alki Point site, fluid samples were also obtained by attaching two additional Niskin bottles to the front of a small commercial Phantom ROV. These Niskin bottles were the traditional non-gas-tight sampling containers. Helium isotope measurements were performed by the NOAA laboratory at PMEL Newport, Oregon (Baumberger et al., 2018; Table T3). Immediately upon recovery of the CTD/Niskin package and the ROV onto the deck of the surface ship, air-free water samples were flushed through 24-inch-long sections of refrigeration grade Cu tubing with duplicate half-sections cold-weld sealed (RC0038) or flushed through 32-inch-long sections of refrigeration grade 3/8 inch OD Cu tubing with a clamp seal (RC0019) for later laboratory analysis (Young & Lupton, 1983). Isotope ratios and concentrations of helium were then determined at the NOAA/PMEL Helium Isotope Laboratory in Newport, OR, USA using a dual collector, 21-cm-radius mass spectrometer with 1σ precision of 0.1%–0.3% in δ^3He, where δ^3He is the percentage deviation of $^3He/^4He$ from the atmospheric ratio, and a concentration accuracy of 1% relative to a laboratory air standard.

2.5. Temperature of the Plume Fluid

A NOAA Miniature Autonomous Plume Recorder (MAPR) with temperature, pressure, turbidity, and negative ion sensors was also attached to the ROV frame for our Kingston and Alki Point cruises (Baker & Milburn, 1997; Walker et al., 2004; Figure 6). No temperature anomalies were detected with the surface ship CTD sensors and only extremely modest +0.005°C to +0.010°C temperature anomalies higher than the adjacent seawater values were observed when the MAPR was deployed directly overlying active vent orifices by the ROV at the Alki Uplift
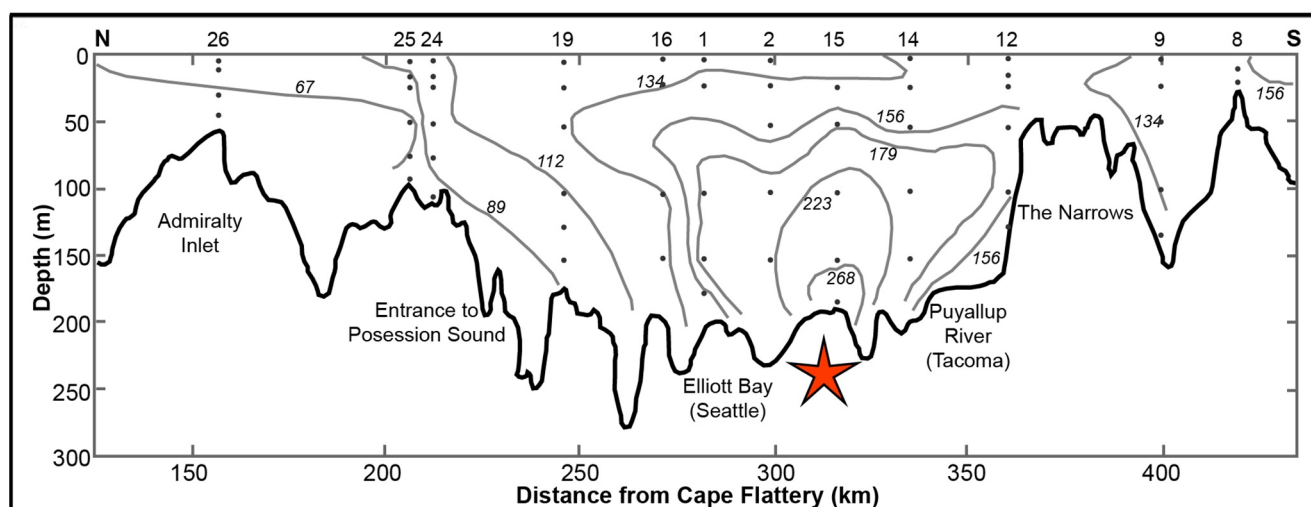
Figure 7. Figure extracted from a 1983 NOAA/PMEL report showing contoured data from a series of CTD casts taken from Admiralty Inlet to South of the Tacoma Narrows (for locations, see Figure 1 and Figure S1 in Supporting Information S1). Dissolved methane concentrations are in units of nM. Small black dots are the positions of the Niskin bottle samples. Red star is approximate position of the Alki Point plume field shown in Figure 1.

field (Figure 6). The temperature resolution of the MAPR is 0.001°C and the time interval occupied for the temperature spikes shown in Figure 6 was approximately 35 s. With a geothermal gradient of approximately 25°C/km present in the Puget Sound forearc region (Blackwell et al., 1990; Salmi et al., 2017), the modest MAPR temperature anomalies indicate that the upwelling vent fluid and gas from the sub-surface must have been in thermal equilibrium with the low temperatures found only in very uppermost 10 cm of seafloor sediments.

2.6. Routine Chemical Nutrients

Chemical analyses were also performed on the CTD/Niskin samples taken over both the Kingston (RC0019) and Alki Point (RC0038) plume fields and included traditional nutrient data including ($Si(OH)_4$, NH_4, $[NO_3]$, and $[NO_2]$). These data are available as a Tables T1 and T2. These data show only normal Puget Sound seawater composed of North Pacific and riverine mixture from estuarine circulation, without any of the chemical concentration anomalies that are routinely observed in forearc plumes within similar tectonic settings (Cruz et al., 2019; Giggenbach et al., 1993; Kusuda et al., 2014; Morikawa et al., 2016; Nakamura et al., 2014). Although Niskin bottles deployed on a CTD wire are not an efficient tool for capturing rising plume fluid, they have been widely and successfully used in both deep-water hydrothermal and continental methane studies. In this study, however, the fluid captured by Niskin bottles appears to be only normal Puget Sound seawater.

2.7. Archive Data

In May of 1980, the newly established Pacific Marine Environmental Laboratory of the National Oceanic and Atmospheric Administration-PMEL began a comprehensive study of particulate and dissolved organic compounds in Puget Sound that included full-depth profiles of dissolved methane that extended from north of Admiralty Inlet to south of the Tacoma Narrows (Curl, 1983). This government document was retrieved from the archives (https://books.google.com.gi/books?id=C_UeAQAAIAAJ&source=gbs_navlinks_s) and Figure 11 of the NOAA report was digitally extracted and the units of dissolved methane obtained from these CTD samples converted from original microliter/liter STP to the standard units of nM using modern Puget Sound temperature and salinity values for the contour labels. This extracted Figure 11 from the NOAA/PMEL report is reproduced here as Figure 7. Although the 1980 sampling track did not pass directly over the Alki Point plume field, the closest point on the 2-D plot is indicated by a red star. The near-surface methane values in this reproduced figure closest to the Alki Point location are substantially higher (134 nM) than those measured by our recent flow-through surface measurements (30 nM) shown in Figure 5 taken 40 years later. This substantial variation in seawater methane concentrations is a relatively common phenomena associated with time-series measurements of methane vents, which can vary

by a factor of 10 on daily, annual, or decadal time scales (Lee & Hautala, 2021; Ola-Dølven et al., 2021; Römer et al., 2016; Salmi et al., 2011).

2.8. Geological Context

Puget Sound is a glacially carved fjord within the forearc plate of the Cascadia Subduction Zone. The estuary forms the southern part of the Salish Sea, which also includes Hood Canal and the Straits of Georgia, which are linked to the North Pacific through the Straits of Juan de Fuca. In the north, Puget Sound is separated from the Straits of Juan de Fuca by a shallow 60-m-deep double sill at Admiralty Inlet, located just north of the Kingston Arch (Figure 1; MacCready et al., 2020; Moore, Mantua, Kellogg, & Newton, 2008, Moore, Mantua, Newton, et al., 2008; Thomson et al., 2007). South of the formal estuary entrance at Admiralty Inlet, Puget Sound covers a surface area of 2,330 km^2, has a length of 182 km, a 16 km maximum width, and a maximum water depth of 280 m. The estuary is geographically separated into individual basins; the North Basin which includes the Main Seattle Basin that extends southward from Admiralty Inlet to Tacoma Narrows, the South Sound located south of the Tacoma Narrows, the semi-isolated Whidbey Basin, which is a land-bounded region located east of Whidbey Island that receives much of the Skagit River inflow, and the adjacent Hood Canal (Figure 1; Figure S1 in Supporting Information S1).

Bathymetrically, these hydrologically interconnected basins are partitioned by prominent shallow sills. Tidal flow over these sills induces turbulence that periodically disrupts the normal estuarine circulation which consists of an upper layer of relatively cold low-salinity riverine-input water flowing northward that overlies the warmer, generally southward-flowing, high-salinity Pacific Ocean water beneath (Cannon et al., 1990; Ianson et al., 2016; Sutherland et al., 2011; Thomson et al., 2007).

The majority of the Puget Sound bubble plume fields are located associated with surface traces of the three major regional fault zones that fracture the northern Cascadia forearc plate. These are the SWIF, the Seattle Fault (SFZ), and the Tacoma Fault Zones (TFZ), which have been well-studied and mapped in considerable detail (Blakely et al., 2002, 2011; Brocher et al., 2000, 2001; Clement et al., 2010; Nelson et al., 2003; Pratt et al., 1997, 2003, 2015; S. Y. Johnson et al., 1994, 1996, 1999, 2004; Sherrod et al., 2000, 2004, 2008). Some of the non-clustered bubble streams also overlie the unnamed North-South trending Seattle Basin Fault described in S. Y. Johnson et al. (1999; Figures 1 and 8b).

These regional fault zones have been proposed to penetrate completely through the North American forearc plate down to the Cascadia Subduction Zone plate interface approximately 43 km below the surface and the specific details of these fault zones extensively discussed in S. Y. Johnson et al. (1994, 1999), Gomberg et al. (2010), Blakely et al. (2011), Sherrod et al. (2000, 2004, 2008), McCrory et al. (2016), and Hyndman et al. (2015) and are only briefly summarized below (Figures 8a and 8b). It is important to note here that there is a significant diversity in interpretations of these fault zones. As an example, published studies supportive of East-West trending cross faults in the Puget Lowland are S. Y. Johnson et al. (1999) and Calvert and Fisher (2001), while other interpretations that do not show the cross faults were published by Blakely et al. (2002), Pratt et al. (2015), and the USGS Active Faults Database (2021). The present study remains agnostic regarding these different interpretations.

The SWIF extends from southern Vancouver Island in the northwest to Seattle in the southeast and has produced at least four Holocene earthquakes with the most recent 2,700 years BP (Sherrod & Gomberg, 2014; Sherrod et al., 2008). This vent field is located on the southern edge of the Kingston Arch anticline which is a broad thinly sedimented anticline that forms the northern boundary of the Seattle Basin (Pratt et al., 1997; S. Y. Johnson et al., 1994; Sherrod & Gomberg, 2014; Sherrod et al., 2008). The eastern submerged portion of the Kingston Arch anticline is the site of an extended linear North-South marine plume field located where the N-S trending fault zone described by S. Y. Johnson et al. (1999) appears to intersect the southern part of the E-W trending SWIF (Figures 1 and 8a). The Kingston Arch anticline is near the junction of these two obliquely intersecting faults and originated as an isolated basin-margin fold that began in the late Eocene and remains seismically active well into the Holocene (Brocher et al., 2001; Mace & Keranen, 2012; Pratt et al., 1997, 2015; S. Y. Johnson et al., 1994, 1996).

The East-West trending SFZ (Figures 1 and 8b) is a south-dipping reverse fault that has over the course of the last 40 My lifted a hanging wall to overlie the Seattle Main Basin that lies immediately to the north. This central Main Seattle Basin is a 10 km deep depression filled with both Oligocene and younger Holocene/Quaternary
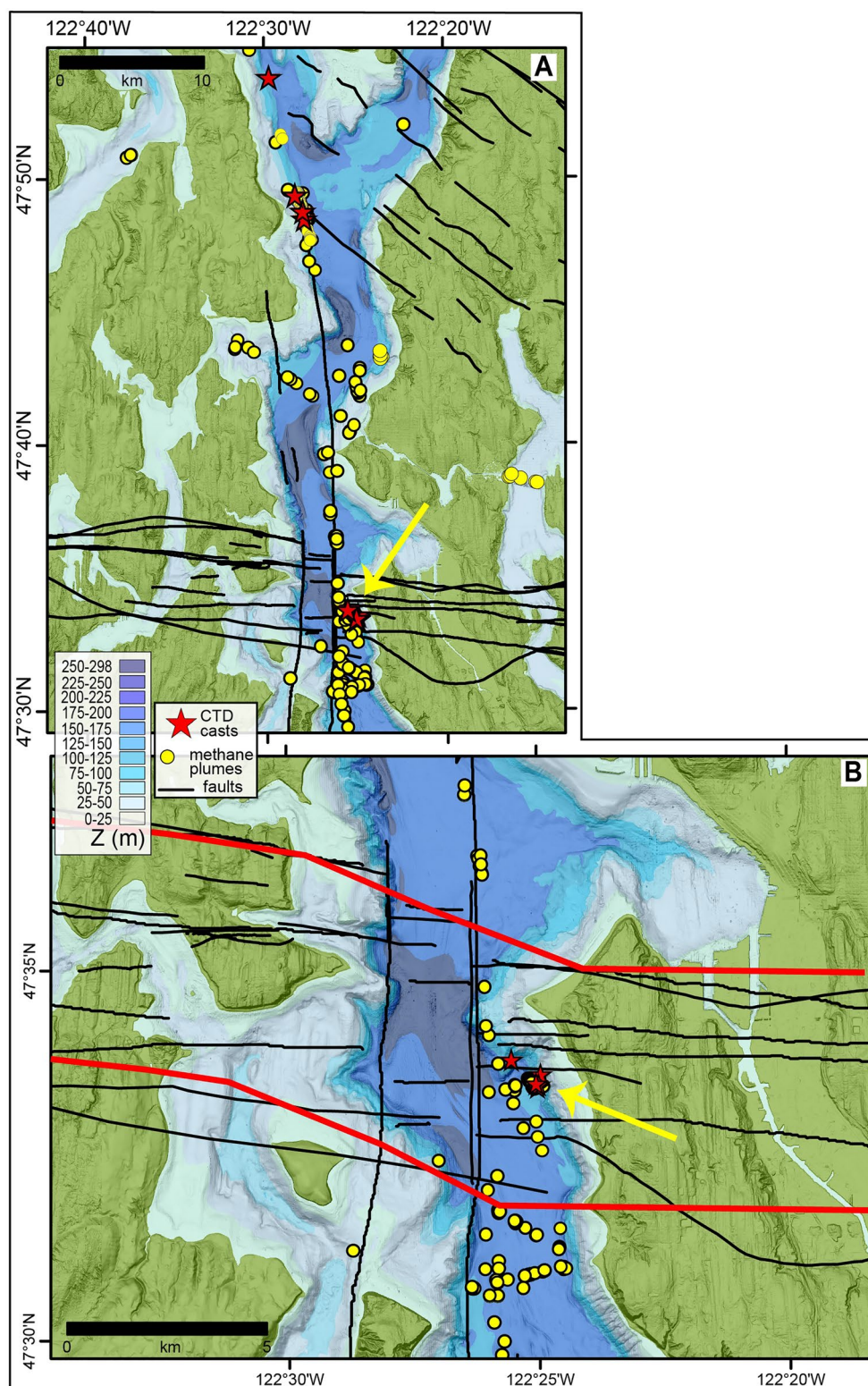
Figure 8. (a) Top left: red stars show locations of CTD casts and yellow arrow points to ROV dive site. Black lines are USGS fault trace compilations with the addition of the N-S S. Y. Johnson et al. (1999) fault lines from multi-channel seismic surveys. Blue regions are seawater and green areas terrestrial. (b) Bottom: expanded view of Alki Uplift site, red stars are CTD casts, yellow arrow points to remotely operated vehicle dive sites. Heavy red lines denote boundaries of the Alki Uplift of U. S. ten Brink et al. (2006). Yellow circles are methane plume sites, showing locations that are both overlying the primary fault traces and also at the fault edges.
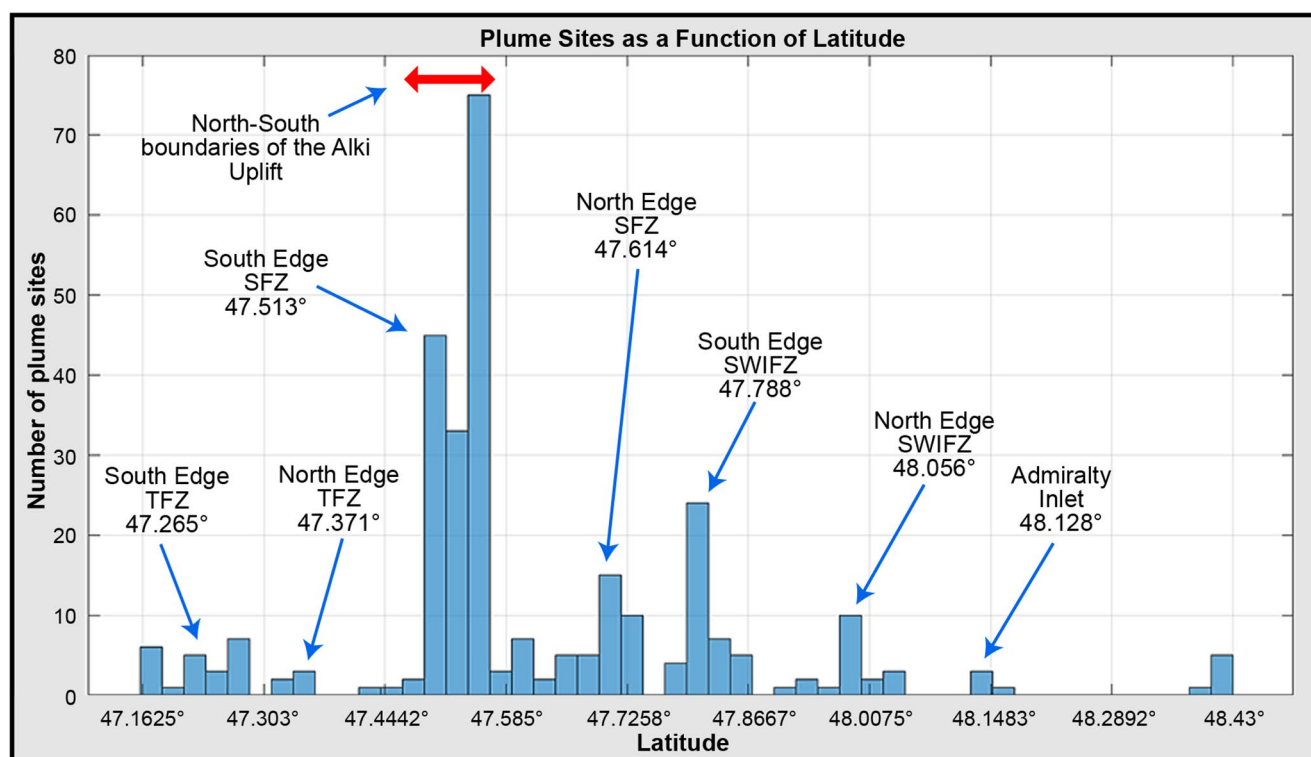
Figure 9. Histogram of plume site frequency with respect to the north-south latitude of the major fault zones, where Tacoma Fault Zones is the Tacoma Fault, Seattle Fault Zone is the Seattle Fault, and SWIFZ are the South Whidbey Island Fault Zones. Admiralty Inlet is the northern boundary of the Puget Sound basins; sites farther north are within the Straits of Juan de Fuca. *Note*. The highest frequencies of plume sites are positioned at the bounding edges of the fault zones, and not within their central regions. The Alki Uplift is a prominent faulted block at the southern edge of the SFZ identified by U. S. ten Brink et al. (2006). Kinston Arch is an uplifted anticline at the boundary of the Southern SWIFZ (S. Y. Johnson et al., 1996). The large number of plume sites at the Alki Uplift is in part a sampling bias due to frequent cruises to that general area.

sediments that can be up to 400 m thick in a few regions (Blakely et al., 2002; Brocher et al., 2001, 2004; Kelsey et al., 2008; Pratt et al., 1997; S. Y. Johnson et al., 1994, 1996, 1999, 2004; U. ten Brink et al., 2002; U. S. ten Brink et al., 2006). The Holocene and Quaternary sediment thickness is extremely variable both along- and across-strike, dramatically thinning over uplifts (i.e., Kingston, Alki Point) and thickening to several 100 m in mid-basin. Relevant to this study, sediment is almost absent at Alki Point where the methane plume fields are dense and their emissions vigorous (Figures 5a and 5c; S. Johnson, pers. comm. 2021; S. Y. Johnson et al., 1999).

The most recent major earthquake on the SFZ was a magnitude M7 about 915 A.D. (Bucknam et al., 1992). During this seismic event, shorelines on southern Bainbridge Island were uplifted by 4 m (Kelsey et al., 2008; Sherrod et al., 2000), with uplift also occurring near Alki Point (Figures 8a, 8b and 9; Kelsey et al., 2008; U. S. ten Brink et al., 2006). The Alki uplift and the broader SFZ experienced approximately 8 m in vertical motion during this earthquake and both the north and south boundaries of this uplifted block at Alki Point are active marine methane vent sites (Figures 8a, 8b and 9; U. S. ten Brink et al., 2006).

Within the Main Seattle Basin where the East-West trending SF is located, S. Y. Johnson et al. (1999) used USGS Multi-Channel Seismic profiles to map a series of north-south trending faults that strike orthogonally across the east-west trending axis of the Seattle Uplift (Figures 8a and 8b). These north-south faults within the Main Seattle Basin are associated with some of the individual isolated plume emission sites that do not appear in clustered fields. Such spatial variability suggests that the active faulting in the Puget Basin may be both more complex and perhaps more abundant than has been previously recognized (Savage & Brodsky, 2011).

The TFZ (Figure 1) is a south-verging thrust fault that is the structural contact between the Main Seattle Basin in the north and South Puget Sound to the south (Blakely et al., 2011; S. Y. Johnson et al., 2004; Sherrod et al., 2004). Trenching of terrestrial fault exposures showed that TFZ active tectonic events occurred in A.D. 770, 900–930, and 1,160 (Sherrod et al., 2004). These geological records of active faulting and lidar-illuminated

terrestrial scarps demonstrate the SWIF, the SFZ, and the TFZ still pose a significant modern seismic hazard to the heavily populated central and southern Puget Sound regions (Sherrod et al., 2004).

Puget Sound sediments have a complex depositional history and include several layers of glacial and inter-glacial sediments beneath the uppermost Holocene and Quaternary layers, while below that are Eocene turbidites, which in turn may rest on the volcanic Eocene Crescent basalts (R. Wells et al., 2014; Rau & Johnson, 1999; S. Y. Johnson et al., 1994). Although poorly sampled, post-glacial Holocene sediments in the uppermost part of the Seattle Basin seafloor consist primarily of clay and silt, with only minor sand (Cochrane et al., 2015; Crecelius et al., 1975; Grundmanis, 1990). S. Y. Johnson et al. (1999, their Figure 3) show that the terrestrial portion of the Puget Basin includes several layers of glacial and inter-glacial sediments at elevations above sea level, which are the terrestrial strata that hosts the water wells and warm springs that tap aquifers with the helium-3 signature (Booth, 1994; McCrory et al., 2016).

The location of the marine methane emission sites overlying deep-seated forearc fault zones initially suggested that gas and fluid could arise from the underlying plate interface of the Cascadia Subduction Zone, as has been noted in terrestrial aquifers that are immediately adjacent to the estuary (McCrory et al., 2016; Figure 1 and Figure S1 in Supporting Information S1). This would be similar to fluid and gas vents located in other global forearcs, where the depth to the plate interface is similar to the 43 km depth beneath Puget Sound (Doğan, et al., 2006; Reynard, 2016). In support of this initial hypothesis, the regional faults that penetrate through the Cascadia forearc crust have been previously proposed as pathways for upward migration of the inter-plate fluid generated from heating along the subduction zone below Puget Sound (Delph et al., 2018; Hyndman et al., 2015; McCrory et al., 2016; R. E. Wells et al., 2017).

R. E. Wells et al. (2017) suggested that over-pressured fluids within the subduction zone interface that are in contact with the underlying oceanic plate are incompletely drained by the regional faults in the forearc and that this partial and episodic fluid drainage controls the temporal segmentation of the 14-month cycle of Episodic Tremor and Slip present in northern Cascadia (Chapman & Melbourne, 2009; Gao & Wang, 2017; Nakajima & Uchida, 2018). The permeability and transport properties of these deep fault conduits in the Cascadia forearc have also been suggested to be episodically enhanced by incident seismic waves from either local or distant earthquakes (Audet & Bürgmann, 2014; Hyndman, et al., 2015; Vidale et al., 2011).

The offsets of the East-West SF traces produced by the North-South along-strike faults of S. Y. Johnson et al. (1999) could provide the high crustal fluid permeability that has been previously observed in both estuarine faults (Naudts et al., 2012) and terrestrial fault zones (Bense et al., 2013; Brixel et al., 2020; Evans et al., 1997; Sibson, 1996; Figures 8a and 8b). The intersection between two faults with different directional trends provides wide fault-damage zones with high permeability that are transport pathways for upwelling crustal fluid (Savage & Brodsky, 2011; Sun et al., 2020). An alternative hypothesis would be for the methane gas and fluid arise from a shallow reservoir within the upper Holocene sediments and transferred laterally by sub-surface horizontal faulting until reaching vertical pathways that overlie the deep regional fault zones (S. Y. Johnson, pers. comm. 2021; Rocha et al., 2021).

3. Results

Abundant multi-channel profiles have examined the sub-seafloor of Puget Sound in both across- and along-strike surveys of the North-South trending topography of the estuary. Correlation of these tectonic features with the locations of bubble plume clusters detected by the RV CARSON single-beam sonar data shows that most of the large multi-plume vent fields are underlain by these deep regional fault zones (Figure 9), and this is particularly evident at the Kingston Arch (SWIF) and SF Uplift fields. As a caveat, the SWIF and SF areas are both located where the MCS profile coverage is extensive, and the bubble plume fields are also well-surveyed by the RV CARSON sonar tracklines, suggesting a probable sampling bias to the emission site distribution.

Some terrestrial-bounded estuaries with very high sedimentation rates have been shown to host methane bubble streams which are not associated with underlying methane reservoirs or permeable fault zones (Judd & Hovland, 2009; Römer et al., 2016). However, gas emissions from sediment pores from these recent estuary deposits require sediment deposition rates that are an order of magnitude higher than the 0.5 cm/year of Puget Sound measurements in the Main Seattle Basin (Judd & Hovland, 2009; Lavelle et al., 1986). Further, limited sampling

shows the uppermost layer of Puget Sound sediments has a well-defined sulfate-methane-transition zone which is depleted in CH_4 and extends to at least a meter in depth in the estuary (Grundmanis, 1990; Sultan et al., 2016).

Puget Sound bottom water is well-flushed tidally and the bottom waters of all three basins are very well-oxygenated (Deppe et al., 2018). Due to methanotrophic bacteria and a well-developed sulfate methane transition zone, the upper sediment layers of the estuary do not appear to be able to produce free-methane bubble streams without being previously accumulated within a sub-surface reservoir. Any vertical gas transfer likely requires transport by way of a pre-existing, perhaps faulted pathway, similar to other methane gas emission sites (Prouty et al., 2020). While several areas in Puget Sound show single isolated bubble streams, most identified gas emission sites are tightly clustered in areas that either overlie the boundaries of the well-mapped regional fault zones (Figure 9) or are distributed along the linear fault traces and are particularly abundant in clusters where fault zones with different geographical orientations intersect.

In dramatic contrast to our expectations derived from other global forearc vents and from the terrestrial aquifer data from water wells and warm springs that permeate the Cascadia forearc (McCrory et al., 2016), our limited Niskin fluid data from the marine bubble plume field showed only normal Puget Sound seawater. Specifically, these samples were composed of Northeast Pacific Ocean seawater mixed with a variable amount of freshwater riverine input (Moore, Mantua, Kellogg, & Newton, 2008; Moore, Mantua, Newton, et al., 2008). Also contrary to our expectations from other subduction-zone forearc vents which exhibit elevated temperatures, only very small thermal anomalies were identified within our limited sampling of Puget Sound plume fields. However, given the resource constraints of this pilot program, it remains possible that more well-positioned samples taken directly from the plume vent orifices might yield different and more satisfying results.

The one unequivocal result is that there is a high abundance of methane bubble plumes within Puget Sound. These plume emissions are spatially correlated with the traces of major fault zones that penetrate deeply into the Cascadia forearc (Figures 1 and 9). However, this limited field program observed (a) extremely small temperature anomalies near the bubble emission sites which indicates that gas provides the prime buoyancy driving the plume flow, (b) normal North Pacific seawater chemistry and salinity for the water samples taken in close proximity to bubble plumes, (c) based on the 1980 and 2021 surveys shown in Figures 5 and 7, methane is the most probable plume gas, and (d) an absence of any helium-3 isotope anomalies indicative of a deep igneous or a mantle-related source region for the plume fluids.

A flow-through seawater analyzer measuring methane concentrations and carbon isotopes in CH_4 show that fluids at the sea surface above the Alki Point plume site have concentrations of methane that are orders of magnitude higher than both North Pacific water and atmospheric abundances (Figure 5). The estuary methane also appears to have carbon isotope ratios weakly consistent with a thermogenic rather than biogenic origin, although oxidation by methanotrophic bacteria within the water column can confuse this bimodal interpretation (Figure 5). Isotopic analysis of both carbon and hydrogen in methane from fluid issuing directly from the seafloor orifice rather than the sea surface would be a far more definitive test, but these samples are not yet available and logistically challenging to obtain.

The correlation of the Puget Sound plume emission sites with the locations of major regional fault zone traces strongly suggests that relatively recent tectonic activity may provide vertical pathways through the upper Holocene sediments recently deposited on the estuary seafloor, which varies widely in thickness within the Basin (S. Y. Johnson et al., 1999). This hypothesis may be valid for plumes located in the middle of the basins, where bubble streams are active - even though the recent sediments can reach several 100 m in thickness in these areas. All three of the regional Puget Basin fault zones are still considered tectonically active (Sherrod et al., 2004, 2008). This tectonic activity may disturb the recent seafloor sediments and generate pathways for an initially deep-seated source of gas of unknown initial composition that is substituted by methane during upward transit through the sediment column (Algar and Boudreau, 2020; Algar et al., 2011; Boudreau, 2012). This model of a deep reservoir for the methane, while initially appealing, is not supported by the temperature or chemistry data of the plume fluid that we sampled and have described above.

The recent limited methane data from surface waters shown in Figure 5 is corroborated by 1980 archive NOAA/PMEL data (Figure 7) that shows that Puget Sound has high methane concentrations throughout the entire estuary and distributed within the entire water column. These concentrations were extremely high in the Main Seattle Basin near Alki Point, where the density of plume emission sites is also high (Figures 8b and 9). The archive 1980

data indicates that the current methane emission sites have been active for decades, and their correlation with presently active emission sites overlying fault zones suggests an even longer-term geological process.

A major unresolved issue is the lack of any chemical or thermal indication of a deep source for the bubble plumes. In Puget Sound, the nearest terrestrial water-well with a mantle helium-3 signature is located on Bainbridge Island (Figure 1). This water-well is only 5 km distant from the nearest Puget Sound bubble plume vent site at Alki Point, and both the terrestrial and marine sites appear to be associated with the same branch of the SFZ (Figure 1). Terrestrial water-wells located near the Kingston Arch plume field have similar helium-3 signatures (Figure 1), suggesting that the helium-3 isotope results from the Bainbridge Island water well is not an isolated phenomenon. The proximity of terrestrial aquifers with clear helium isotope anomalies, identified on the same fault traces as the marine plume sites suggests but certainly does not prove, that the terrestrial and marine fluids could perhaps arise from a common sub-surface reservoir, but without a common helium-3 signature. This presents an unresolved paradox that requires additional study.

4. Conclusions and the Paths Forward

Puget Sound contains an unexpectedly large number of methane bubble plumes that, along with a yet-unmeasured seasonal riverine input, maintain a high level of methane supersaturation with respect to the atmosphere. Extensive single-beam sonar surveys by the RV CARSON show that the bubble plume sites are distributed throughout the Sound, with clustered fields that are concentrated near three major regional fault zones. Although Puget Sound lies within the Cascadia Subduction Zone forearc and these regional fault zones appear to penetrate deeply into the forearc plate, our new data appears to strongly suggest a much shallower source region may be responsible for the methane plume gas and fluid.

Our limited Puget Sound plume chemistry does not support the hypothesis of a direct origin of the vent bubbles arising directly from the underlying Cascadia subduction zone plate interface. The low temperatures of the fluid also seem to exclude even a shallower sub-surface igneous rock reservoir such as the Siletz Terrain (R. E. Wells et al., 2017). We acknowledge that our data are incomplete, and our preliminary sampling and analysis of vent fluids are too limited to provide confirmation of any satisfying hypothesis. However, the presence of at least 349 individual methane bubble plumes within the Puget Sound forearc associated with the major deep-seated fault systems that penetrate the forearc crust merits presentation to the wider scientific community to provide context for more complete further studies.

Without more definitive data, a wide range of alternative explanations for the bubble plumes exists and a more compelling and satisfying hypothesis may be confirmed by subsequent field programs. Primarily these future field programs would include better methods for vent fluid sampling, more extensive chemical analyses, and high-resolution seismic imaging of the vent fields (Sassen et al., 2003). Comprehensive sampling programs of emission fluid chemistry at a wider range of marine sites, including the Kingston Arch field and the plumes located in the deeper, more thickly sedimented mid-basins. Additional sampling and chemical analysis of the three terrestrial water wells that show mantle helium-3 isotope signatures and are located adjacent to the marine vents could be helpful (i.e., on Bainbridge Island and west of Kington; Figure 1). These sampling programs could determine if the terrestrial wells and the marine vents originate from the same subsurface source area and use similar migration pathways. Systematic long-term time-series measurements of the bubble emission flux could be correlated with external forcing including earth and seawater tidal forcing, storm surges, the 14-month cycle of Episodic Tremor and Slip events and/or the passage of distant seismic waves. These forcing processes have been shown elsewhere to modulate vent flow and therefore provide considerable insight regarding the depth of the source area and the properties of the transport pathways.

Some possible alternatives for the marine plume source include spring sapping flow from terrestrial reservoirs that are adjacent to the subseafloor aquifer (Brooks et al., 2021), the presence of an undetected/unrecognized sub-seafloor fluid reservoir beneath Puget Sound (Morikawa et al., 2016; Tauzin et al., 2017), or simple vertical compression of the seafloor sediments (Wang et al., 2018) where the extruded fluid migrates horizontally and then upward through disturbed sediment pathways defined by movement along the regional faults. Our data does not support or negate any of these hypotheses.

However, in spite of the limitations of this study, one observation remains. Puget Sound, an estuary within the deeply fractured forearc plate of the Cascadia Subduction Zone, hosts an abundance of methane gas plumes that correlate with these regional fault zones (Figure 9). Although the flux of methane emission from these plumes still remains unquantified, comparison with other continental margin vent sites suggests that the methane from the plumes may strongly impact the general biological and chemical environment of the Puget Basin, as similar plumes do elsewhere (Jordan et al., 2020; Schubert et al., 2006). As the methane-rich seawater of the Sound is eventually discharged by estuarine circulation through the Straits of Juan de Fuca into the coastal NE Pacific, the influence of these bubble plumes, generated within a large inland sea, may potentially extend farther west, into a far wider environment.

Conflict of Interest

The authors declare no conflicts of interest relevant to this study.

Data Availability Statement

Data supporting this study can be found in Supporting Information and are also available online in the Zenodo database repository as doi:10.5281/zenodo.5775137. The files, tables, and text listed below are included as Supporting Information. The RV CARSON 38 kHz sonar data is available from the NSF Rolling-Deck-to-Repository archives and available by RV CARSON cruise number as listed in the Supporting Information Text.

References

Algar, C. K., & Boudreau, B. P. (2020). Stability of bubbles in a linear elastic medium: Implications for bubble growth in marine sediments. *Journal of Geophysical Research: Earth Surface*, *115*, F3. https://doi.org/10.1029/2009JF001312

Algar, C. K., Boudreau, B. P., & Barry, M. A. (2011). Initial rise of bubbles in cohesive sediments by a process of viscoelastic fracture. *Journal of Geophysical Research*, *116*(B4). https://doi.org/10.1029/2010jb008133

Angster, S. J., Sherrod, B., Barnett, E., Bretthauer, J. L., & Anderson, M. L. (2020). *Update to the quaternary Fault and fold database for Washington State*. U.S. Geological Survey data release. https://doi.org/10.5066/P9X2RR2T

Audet, P., & Bürgmann, R. (2014). Possible control of subduction zone slow-earthquake periodicity by silica enrichment. *Nature*, *510*(7505389). https://doi.org/10.1038/nature13391

Baker, E. T. & Milburn, H. B. Miniature Autonomous PlumeRecorders (MAPR). https://www.pmel.noaa.gov/eoi/PlumeStudies/mapr/

Baumberger, T., Embley, R. W., Merle, S. G., Lilley, M. D., Raineault, N. A., & Lupton, J. E. (2018). Mantle-derived helium and multiple methane sources in gas bubbles of cold seeps along the Cascadia continental margin. *Geochemistry, Geophysics, Geosystems*, *19*, 4476–4486. https://doi.org/10.1029/2018GC007859

Bense, V. F., Tom Gleeson, S. E. L., Olivier, B., & Scibek, J. (2013). Fault zone hydrogeology. *Earth-Science Reviews*, *127*, 171–192. https://doi.org/10.1016/j.earscirev.2013.09.008

Blackwell, D. D., Steele, J. L., Kelley, S., & Korosec, M. A. (1990). Heat flow in the state of Washington and thermal conditions in the Cascade Range. *Journal of Geophysical Research*, *95*(B12), 19495–19516. https://agupubs.onlinelibrary.wiley.com/doi/abs/10.1029/JB095iB12p19495

Blakely, R. J., Sherrod, B. L., Weaver, C. S., Wells, R. E., Rohay, A. C., Barnett, E. A., & Knepprath, N. E. (2011). Connecting the Yakima fold and thrust belt to active faults in the Puget Lowland, Washington. *Journal of Geophysical Research*, *116*(B7). https://doi.org/10.1029/2010jb008091

Blakely, R. J., Wells, R. E., Weaver, C. S., & Johnson, S. Y. (2002). Location, structure, and seismicity of the Seattle fault zone, Washington: Evidence from aeromagnetic anomalies, geologic mapping, and seismic-reflection data. *The Geological Society of America Bulletin*, *114*(2), 169–177. https://doi.org/10.1130/0016-7606(2002)114<0169:LSASOT>2.0.CO;2

Boetius, A., & Wenzhöfer, F. (2013). Seafloor oxygen consumption fuelled by methane from cold seeps. *Nature Geoscience*, *6*(9), 725–734. https://doi.org/10.1038/ngeo1926

Booth, D. B. (1994). Glaciofluvial infilling and scour of the Puget Lowland, Washington, during ice-sheet glaciation. *Geology*, *22*, 695–698. https://doi.org/10.1130/0091-7613(1994)022%3C0695:giasot%3E2.3.co;2

Boudreau, B. P. (2012). The physics of bubbles in surficial, soft, cohesive sediments. *Marine and Petroleum Geology*, *38*(1), 1–18. https://doi.org/10.1016/j.marpetgeo.2012.07.002

Brixel, B., Klepikova, M., Jalali, M. R., Lei, Q., Roques, C., Kriestch, H., & Simon, L. (2020). Tracking fluid flow in shallow crustal Fault Zones: 1. Insights from single-hole permeability estimates. *Journal of Geophysical Research: Solid Earth*, *125*(4), e2019JB018200. https://doi.org/10.1029/2019jb018200

Brocher, T. M., Blakely, R. J., & Wells, R. E. (2004). Interpretation of the Seattle uplift, Washington, as a passive-roof duplex. *Bulletin of the Seismological Society of America*, *94*(4), 1379–1401. https://doi.org/10.1785/012003190

Brocher, T. M., Parsons, T., Blakely, R. J., Christensen, N. I., Fisher, M. A., & Wells, R. E. (2001). Upper crustal structure in Puget Lowland, Washington: Results from the 1998 seismic hazards investigation in Puget sound. *Journal of Geophysical Research*, *106*(B7), 13541–13564. https://doi.org/10.1029/2001jb000154

Brocher, T. M., Pratt, T. L., Creager, K. C., Crosson, R. S., Steele, W. P., Weaver, C. S., et al. (2000). Urban seismic experiments investigate Seattle fault and basin. *Eos, Transactions American Geophysical Union*, *81*(46), 545–552. https://doi.org/10.1029/eo081i046p00545-01

Brooks, T., Kroeger, K. D., Holly, A. M., & JoannaYork, K. (2021). Oxygen-controlled recirculating seepage meter reveals extent of nitrogen transformation in discharging coastal groundwater at the aquifer–estuary interface. *Limnology & Oceanography*. https://doi.org/10.1002/lno.11858

Bucknam, R. C., Hemphill-Haley, E., & Leopold, E. B. (1992). Abrupt uplift within the past 1700 years at southern Puget Sound, Washington. *Science*, *258*(5088), 1611–1614. https://doi.org/10.1126/science.258.5088.1611

Calvert, A. J., & Fisher, M. A. (2001). Imaging the Seattle fault zone with high-resolution seismic tomography. *Geophysical Research Letters*, *28*(12), 2337–2340. https://doi.org/10.1029/2000gl012778

Cannon, G. A., Holbrook, J. R., & Pashinski, D. J. (1990). Variations in the onset of bottom-water intrusions over the entrance sill of a fjord. *Estuaries*, *13*(1), 31–42. https://doi.org/10.2307/1351430

Chapman, J. S., & Melbourne, T. I. (2009). Future Cascadia megathrust rupture delineated by episodic tremor and slip. *Geophysical Research Letters*, *36*(22). https://doi.org/10.1029/2009gl040465

Clement, C. R., Pratt, T. L., Holmes, M. L., & Sherrod, B. L. (2010). High-resolution seismic reflection imaging of growth folding and shallow faults beneath the southern Puget Lowland, Washington State. *Bulletin of the Seismological Society of America*, *100*(4), 1710–1723. https://doi.org/10.1785/0120080306

Cochrane, G. R., Dethier, M. N., Hodson, T. O., Kull, K. K., Golden, N. E., Ritchie, A. C., et al. (2015). *Southern Salish Sea Habitat Map Series: Admiralty Inlet. No. 2015-1073*. US Geological Survey. https://doi.org/10.3133/ofr20151073

Crecelius, E. A., Bothner, M. H., & Carpenter, R. (1975). Geochemistries of arsenic, antimony, mercury, and related elements in sediments of Puget Sound. *Environmental Science & Technology*, *9*(4), 325–333. https://doi.org/10.1021/es60102a007

Cruz, B., Yosvanis, R., Rizzo, A. L., Grassa, F., Romero, R. B., Fernández, A. G., et al. (2019). Mantle degassing through continental crust triggered by active faults: The case of the Baja California Peninsula, Mexico. *Geochemistry, Geophysics, Geosystems*, *20*(4), 1912–1936. https://doi.org/10.1029/2018gc007987

Curl, H. C. (1983). *Summary Report Fiscal Year, Geochemistry, 1982*. Pacific Marine Environmental Laboratory. Retrieved from https://books.google.com.gi/books?id=C_UeAQAAIAAJ&source=gbs_navlinks_s

de Angelis, M. A., & Lilley, M. D. (1987). Methane in surface waters of Oregon estuaries and rivers 1. *Limnology & Oceanography*, *32*(3), 716–722. https://doi.org/10.4319/lo.1987.32.3.0716

Delph, J. R., Levander, A., & Niu, F. (2018). Fluid controls on the heterogeneous seismic characteristics of the Cascadia margin. *Geophysical Research Letters*, *45*(20), 11–021. https://doi.org/10.1029/2018gl079518

Deppe, R. W., Thomson, J., Polagye, B., & Krembs, C. (2018). Predicting deep water intrusions to Puget Sound, WA (USA), and the seasonal modulation of dissolved oxygen. *Estuaries and Coasts*, *41*(1), 114–127. https://doi.org/10.1007/s12237-017-0274-6

Doğan, T., Sumino, H., Nagao, K., & Notsu, K. (2006). Release of mantle helium from forearc region of the Southwest Japan arc. *Chemical Geology*, *233*(3–4), 235–248. https://doi.org/10.1016/j.chemgeo.2006.03.008

Embley, R., Raineault, N., Merle, S., Baumberger, T., Seabrook, S., & Hammond, S. (2017). Water column and cold seep exploration of the Cascadia margin. *Oceanography, Frontiers in Ocean Exploration Supplement*, *30*, 28–30. https://doi.org/10.1130/ges00648.1

Etiope, G. (2012). Climate science: Methane uncovered. *Nature Geoscience*, *5*, 373. https://doi.org/10.1038/ngeo1483

Evans, J. P., Forster, C. B., & Goddard, J. V. (1997). Permeability of fault-related rocks, and implications for hydraulic structure of fault zones. *Journal of Structural Geology*, *19*(11), 1393–1404. https://doi.org/10.1016/s0191-8141(97)00057-6

Frankignoulle, M., Borges, A., & Biondo, R. (2001). A new design of equilibrator to monitor carbon dioxide in highly dynamic and turbid environments. *Water Research*, *35*, 1344–1347. https://doi.org/10.1016/S0043-1354(00)00369-9

Fu, X., Waite, W. F., & Ruppel, C. D. (2020). Hydrate formation on marine seep bubbles and the implications for water column methane dissolution. *Journal of Geophysical Research: Oceans*, e2021JC017363. https://doi.org/10.1029/2021JC017363

Gao, X., & Wang, K. (2017). Rheological separation of the megathrust seismogenic zone and episodic tremor and slip. *Nature*, *543*(7645), 416–419. https://doi.org/10.1038/nature21389

Garcia-Tigreros, F., Leonte, M., Ruppel, C., Ruiz-Angulo, A., Dong, J. J., Young, B., et al. (2020). Estimating the impact of seep methane oxidation on ocean pH and dissolved inorganic radiocarbon along the US mid-Atlantic Bight. *Journal of Geophysical Research: Biogeosciences*, e2019JG005621. https://doi.org/10.1029/2019JG005621

Giggenbach, W. F., Sano, Y., & Wakita, H. (1993). Isotopic composition of helium, and CO_2 and CH_4 contents in gases produced along the New Zealand part of a convergent plate boundary. *Geochimica et Cosmochimica Acta*, *57*(14), 3427–3455. https://doi.org/10.1016/0016-7037(93)90549-c

Gomberg, J., Brian Sherrod, Weaver, C., & Frankel, A. (2010). *A magnitude 7.1 earthquake in the Tacoma Fault zone—A Plausible Scenario for the Southern Puget Sound Region*. US Geological Survey. https://doi.org/10.3133/fs20103023

Grundmanis, V. (1990). *A study of the oxidation of organic matter in pelagic and near-shore sedimentary environments* (PhD thesis, pp. 3355). University of Washington, Seattle.

Hautala, S. L., Solomon, E. A., Johnson, H. P., Harris, R. N., & Miller, U. K. (2014). Dissociation of Cascadia margin gas hydrates in response to contemporary ocean warming. *Geophysical Research Letters*, *41*(23), 8486–8494. https://doi.org/10.1002/2014gl061606

Hornafius, J. S., Quigley, D., & Luyendyk, B. P. ((1999). The world's most spectacular marine hydrocarbon seeps (Coal Oil Point, Santa Barbara Channel, California): Quantification of emissions. *Journal of Geophysical Research*, *104*, 20703–20711. https://doi.org/10.1029/1999JC900148

Hovland, M., & Judd, A. G. (1992). The global production of methane from shallow submarine sources. *Continental Shelf Research*, *12*(10), 1231–1238. https://doi.org/10.1016/0278-4343(92)90082-u

Hyndman, R. D., McCrory, P. A., Wech, A., Kao, H., & Ague, J. (2015). Cascadia subducting plate fluids channelled to fore-arc mantle corner: ETS and silica deposition. *Journal of Geophysical Research: Solid Earth*, *120*(6), 4344–4358. https://doi.org/10.1002/2015jb011920

Ianson, D., Allen, S. E., Moore-Maley, B. L., Johannessen, S. C., & Macdonald, R. W. (2016). Vulnerability of a semi enclosed estuarine sea to ocean acidification in contrast with hypoxia. *Geophysical Research Letters*, *43*(11), 5793–5801. https://doi.org/10.1002/2016gl068996

Johnson, H. P., Merle, S., Salmi, M., Embley, R., Sampaga, E., & Lee, M. (2019). Anomalous concentration of methane emissions at the continental shelf edge of the northern Cascadia Margin. *Journal of Geophysical Research: Solid Earth*, *124*(3), 2829–2843. https://doi.org/10.1029/2018jb016453

Johnson, S. Y., Blakely, R. J., Stephenson, W. J., Dadisman, S. V., & Fisher, M. A. (2004). Active shortening of the Cascadia forearc and implications for seismic hazards of the Puget Lowland. *Tectonics*, *23*(1). https://doi.org/10.1029/2003tc001507

Johnson, S. Y., Dadisman, S. V., Childs, J. R., & Stanley, W. D. (1999). Active tectonics of the Seattle fault and central Puget Sound, Washington—Implications for earthquake hazards. *The Geological Society of America Bulletin*, *111*(7), 1042–1053. https://doi.org/10.1130/0016-7606(1999)111<1042:atotsf>2.3.co;2

Johnson, S. Y., Potter, C. J., & Armentrout, J. M. (1994). Origin and evolution of the Seattle fault and Seattle basin, Washington. *Geology*, *22*(1), 71–74. https://doi.org/10.1130/0091-7613(1994)022<0071:oaeots>2.3.co;2

Johnson, S. Y., Potter, C. J., Armentrout, J. M., Miller, J. J., Finn, C., & Weaver, C. S. (1996). The southern Whidbey Island Fault: An active Structure in the Puget Lowland, Washington. *Geological Society of America Bulletin*, *108*, 334–354. https://doi.org/10.1130/0016-7606(1996)108<0334:tswifa>2.3.co;2

Jordan, S. F. A., Treude, T., Leifer, I., Janßen, R., Werner, J., Schulz-Vogt, H., & Oliver, S. (2020). Bubble-mediated transport of benthic microor-ganisms into the water column: Identification of methanotrophs and implication of seepage intensity on transport efficiency. *Scientific Reports*, *10*(1), 1–15. https://doi.org/10.1038/s41598-020-61446-9

Judd, A., & Hovland, M. (2009). *Seabed fluid flow: The impact on geology, biology, and the marine environment*. Cambridge University Press. https://doi.org/10.1017/CBO9780511535918

Kelsey, H. M., Sherrod, B. L., Nelson, A. R., & Brocher, T. M. (2008). Earthquakes generated from bedding plane-parallel reverse faults above an active wedge thrust, Seattle fault zone. *The Geological Society of America Bulletin*, *120*(11–12), 1581–1597. https://doi.org/10.1130/b26282.1

Kusuda, C., Iwamori, H., Nakamura, H., Kazahaya, K., & Morikawa, N. (2014). Arima hot spring waters as a deep-seated brine from subducting slab. *Earth Planets and Space*, *66*(1), 119. https://doi.org/10.1186/1880-5981-66-119

Ladroit, Y., Escobar-Flores, P. C., Schimel, A. C. G., & O'Driscoll, R. L. (2020). ESP3: An open-source software for the quantitative processing of hydro-acoustic data. *Software*, *12*, 100581. https://doi.org/10.1016/j.softx.2020.100581

Lavelle, J. W., Massoth, G. J., & Crecelius, E. A. (1986). Accumulation rates of recent sediments in Puget Sound, Washington. *Marine Geology*, *72*(1–2), 59–70. https://doi.org/10.1016/0025-3227(86)90099-x

Lee, B. Y., & Hautala, S. L. (2021). Understanding the long-term tidal modulation on methane bubble emissions using acoustics, Southern hy-drate Ridge, Cascadia. *Journal of Advanced Geospatial Science & Technology*, *1*(1), 70–88.

Leifer, I. (2010). Characteristics and scaling of bubble plumes from marine hydrocarbon seepage in the Coal Oil Point seep field. *Journal of Geophysical Research*, *115*(C11). https://doi.org/10.1029/2009jc005844

Leifer, I., & MacDonald, I. (2003). Dynamics of the gas flux from shallow gas hydrate deposits: Interaction between oily hydrate bubbles and the oceanic environment. *Earth and Planetary Science Letters*, *210*(3–4), 411–424. https://doi.org/10.1016/s0012-821x(03)00173-0

Leifer, I., & Patro, R. K. (2002). The bubble mechanism for methane transport from the shallow seabed to the surface: A review and sensitivity study. *Continental Shelf Research*, *22*(16), 2409–2428. https://doi.org/10.1016/s0278-4343(02)00065-1

MacCready, P., McCabe, R. M., Siedlecki, S. A., Lorenz, M., Giddings, S. N., Bos, J., et al. (2020). Estuarine circulation, mixing, and Residence times in the Salish Sea. *Journal of Geophysical Research: Oceans*, e2020JC016738. https://doi.org/10.1029/2020JC016738

Mace, C. G., & Keranen, K. M. (2012). Oblique fault systems crossing the Seattle basin: Geophysical evidence for additional shallow fault sys-tems in the central Puget Lowland. *Journal of Geophysical Research*, *117*(B3). https://doi.org/10.1029/2011jb008722

Mau, S., Gentz, T., Körber, J.-H., Torres, M. E., Römer, M., Sahling, H., et al. (2015). Seasonal methane accumulation and release from a gas emission site in the central North Sea. *Biogeosciences*, *12*(18). https://doi.org/10.5194/bg-12-5261-2015

Mau, S., Heintz, M. B., & Valentine, D. L. (2012). Quantification of CH_4 loss and transport in dissolved plumes of the Santa Barbara Channel, California. *Continental Shelf Research*, *32*, 110–120. https://doi.org/10.1016/j.csr.2011.10.016

McCrory, P. A., Constantz, J. E., Hunt, A. G., & Blair, J. L. (2016). Helium as a tracer for fluids released from Juan de Fuca lithosphere beneath the Cascadia forearc. *Geochemistry, Geophysics, Geosystems*, *17*(6), 2434–2449. https://doi.org/10.1002/2015gc006198

Merle, S. G., Embley, R. W., Johnson, H. P., Lau, T.-K., Phrampus, B. J., Raineault, N. A., & Gee, L. J. (2021). Distribution of methane Plumes on Cascadia margin and implications for the landward limit of methane hydrate stability. *Frontiers of Earth Science*, *9*, 531714. https://doi.org/10.3389/feart.2021.531714

Moore, S. K., Mantua, N. J., Kellogg, J. P., & Newton, J. A. (2008). Local and large-scale climate forcing of Puget Sound oceanographic proper-ties on seasonal to interdecadal timescales. *Limnology & Oceanography*, *53*(5), 1746–1758. https://doi.org/10.4319/lo.2008.53.5.1746

Moore, S. K., Mantua, N. J., Newton, J. A., Kawase, M., Warner, M. J., & Kellogg, J. P. (2008). A descriptive analysis of temporal and spa-tial patterns of variability in Puget Sound oceanographic properties. *Coastal and Shelf Science*, *80*(4), 545–554. https://doi.org/10.1016/j.ecss.2008.09.016

Morikawa, N., Kazahaya, K., Takahashi, M., Inamura, A., Takahashi, H. A., Yasuhara, M., & Ohwada, M. (2016). Widespread distribution of ascending fluids transporting mantle helium in the fore-arc region and their upwelling processes: Noble gas and major element composition of deep groundwater in the Kii Peninsula, southwest Japan. *Geochimica et Cosmochimica Acta*, *182*, 173–196. https://doi.org/10.1016/j.gca.2016.03.017

Nakajima, J., & Uchida, N. (2018). Repeated drainage from megathrusts during episodic slow slip. *Nature Geoscience*, *11*(5), 351–356. https://doi.org/10.1038/s41561-018-0090-z

Nakamura, H., Fujita, Y., Nakai, S., Yokoyama, T., & Iwamori, H. (2014). Rare earth elements and Sr–Nd–Pb isotopic analyses of the Arima hot spring waters, Southwest Japan: Implications for origin of the Arima-type brine. *Journal of Geophysical Research*, *3*, 2–161. https://doi.org/10.4172/2329-6755.1000161

Naudts, L., Khlystov, O., Granin, N., Alexander, C., Poort, J., & De Batist, M. (2012). Stratigraphic and structural control on the distribution of gas hydrates and active gas seeps on the Posolsky Bank, Lake Baikal. *Geo-Marine Letters*, *32*(5–6), 395–406. https://doi.org/10.1007/s00367-012-0286-y

Nelson, A. R., Johnson, S. Y., KelseyWells, H. M. R. E., Sherrod, B. L., Pezzopane, S. K., Bradley, L.-A., et al. (2003). Late Holocene earthquakes on the Toe Jam Hill fault, Seattle Fault zone, Bainbridge Island, Washington. *The Geological Society of America Bulletin*, *115*(11), 1388–1403. https://doi.org/10.1130/b25262.1

Nittrouer, C. A., & Sternberg, R. W. (1975). The fate of a fine-grained dredge spoils deposit in a tidal channel of Puget Sound, Washington. *Journal of Sedimentary Research*, *45*(1), 160–170. https://doi.org/10.1306/212f6cf8-2b24-11d7-8648000102c1865d

Ola-Dølven, K., Ferré, B., Silyakova, A., Jansson, P., Peter, L., & Moser, M. (2021). Autonomous methane seep site monitoring offshore Western Svalbard: Hourly to seasonal variability and associated oceanographic parameters. *Ocean Science Discussions*, 1–31. https://doi.org/10.5194/os-2021-85,

Pack, M. A., Heintz, M. B., Reeburgh, W. S., Trumbore, S. E., Valentine, D. L., Xu, X., & EllenDruffel, R. M. (2015). Methane oxidation in the eastern tropical North Pacific Ocean water column. *Journal of Geophysical Research: Biogeosciences*, *120*(6), 1078–1092. https://doi.org/10.1002/2014jg002900

Plaza-Faverola, A., & Keiding, M. (2019). Correlation between tectonic stress regimes and methane seepage on the western Svalbard margin. *Solid Earth*, *10*(1), 79–94. https://doi.org/10.5194/se-10-79-2019

Pratt, T. L., Brocher, T. M., Weaver, C. S., Creager, K. C., Snelson, C. M., Crosson, R. S., et al. (2003). Amplification of seismic waves by the Seattle basin, Washington State. *Bulletin of the Seismological Society of America*, *93*(2), 533–545. https://doi.org/10.1785/0120010292

Pratt, T. L., Johnson, S., Potter, C., Stephenson, W., & Finn, C. (1997). Seismic reflection images beneath Puget Sound, western Washing-ton state: The Puget Lowland thrust sheet hypothesis. *Journal of Geophysical Research: Solid Earth*, *102*(B12), 27469–27489. https://doi.org/10.1029/97JB01830

Pratt, T. L., KathyTroost, G., Odum, J. K., & Stephenson, W. J. (2015). Kinematics of shallow backthrusts in the Seattle fault zone, Washington State. *Geosphere*, *11*(6), 1948–1974. https://doi.org/10.1130/ges01179.1

Prouty, N. G., Brothers, D. S., Kluesner, J. W., Vaughn Barrie, J., Andrews, B. D., Lauer, R. M., & Greene, H. G. (2020). Focused fluid flow and methane venting along the Queen Charlotte fault, offshore Alaska (USA) and British Columbia (Canada). *Geosphere*, *16*(6), 1336–1357. https://doi.org/10.1130/ges02269.1

Rau, W. W., & Johnson, S. Y. (1999). *Well stratigraphy and correlations, western Washington and northwest Oregon: U.S. Geological Survey Map I-2621, 3 oversized sheets/charts* (p. 31).

Razaz, M., Di Iorio, D., Wang, B., Daneshgar Asl, S., & Thurnherr, A. M. (2020). Variability of a natural hydrocarbon seep and its connection to the ocean surface. *Scientific Reports*, *10*(1), 1–13. https://doi.org/10.1038/s41598-020-68807-4

Reynard, B. (2016). Mantle hydration and Cl-rich fluids in the subduction forearc. *Progress in Earth and Planetary Science*, *3*(1), 9. https://doi.org/10.1186/s40645-016-0090-9

Riedel, M., Scherwath, M., Römer, M., Veloso, M., Heesemann, M., & Spence, G. D. (2018). Distributed natural gas venting offshore along the Cascadia margin. *Nature Communications*, *9*(1), 1–14. https://doi.org/10.1038/s41467-018-05736-x

Rocha, L. A. M., Gutiérrez-Ariza, C., Pimentel, C., Sánchez-Almazo, I., Ignacio Sainz-Díaz, C., Cardoso, S. S. S., & HE Cartwright, J. (2021). Formation and structures of horizontal submarine fluid conduit and venting systems associated with marine seeps. *Geochemistry, Geophysics, Geosystems*, e2021GC009724. https://doi.org/10.1029/2021gc009724

Römer, M., Riedel, M., Scherwath, M., Heesemann, M., & Spence, G. D. (2016). Tidally controlled gas bubble emissions: A comprehensive study using long-term monitoring data from the NEPTUNE cabled observatory offshore Vancouver Island. *Geochemistry, Geophysics, Geosystems*, *17*(9), 3797–3814. https://doi.org/10.1002/2016GC006528

Rosentreter, J. A., Borges, A. V., Deemer, B. R., Holgerson, M. A., Liu, S., Song, C., & Melack, J. (2021). Half of global methane emissions come from highly variable aquatic ecosystem sources. *Nature Geoscience*, *14*(4), 225–230. https://doi.org/10.1038/s41561-021-00715-2

Ruppel, C. D., & Kessler, J. D. (2017). The interaction of climate change and methane hydrates. *Reviews of Geophysics*, *55*(1), 126–168. https://doi.org/10.1002/2016rg000534

Salmi, M. S., Paul Johnson, H., & Harris, R. N. (2017). Thermal environment of the Southern Washington region of the Cascadia subduction zone. *Journal of Geophysical Research: Solid Earth*, *122*(8), 5852–5870. https://doi.org/10.1002/2016jb013839

Salmi, M. S., Paul Johnson, H., Leifer, I., & Keister, J. E. (2011). Behavior of methane seep bubbles over a pockmark on the Cascadia continental margin. *Geosphere*, *7*(6), 1273–1283. https://doi.org/10.1130/ges00648.1

Sassen, R., Milkov, A. V., Ozgul, E., Roberts, H. H., Hunt, J. L., Beeunas, M. A., et al. (2003). Gas venting and subsurface charge in the Green Canyon area, Gulf of Mexico continental slope: Evidence of a deep bacterial methane source? *Organic Geochemistry*, *34*(10), 1455–1464. https://doi.org/10.1016/s0146-6380(03)00135-9

Savage, H. M., & Brodsky, E. E. (2011). Collateral damage: Evolution with displacement of fracture distribution and secondary fault strands in fault damage zones. *Journal of Geophysical Research*, *116*(B3). https://doi.org/10.1029/2010jb007665

Schubert, C. J., Durisch-Kaiser, E., Holzner, C. P., Klauser, L., Wehrli, B., Schmale, O., et al. (2006). Methanotrophic microbial communities associated with bubble plumes above gas seeps in the Black Sea. *Geochemistry, Geophysics, Geosystems*, *7*(4). https://doi.org/10.1029/2005gc001049

Sherrod, B., & Gomberg, J. (2014). Crustal earthquake triggering by pre-historic great earthquakes on subduction zone thrusts. *Journal of Geophysical Research: Solid Earth*, *119*(2), 1273–1294. https://doi.org/10.1002/2013jb010635

Sherrod, B. L., Blakely, R. J., Weaver, C. S., Kelsey, H. M., Barnett, E., Liberty, L., et al. (2008). Finding concealed active faults: Extending the southern Whidbey Island Fault across the Puget Lowland, Washington. *Journal of Geophysical Research*, *113*(B5). https://doi.org/10.1029/2007jb005060

Sherrod, B. L., Brocher, T. M., Weaver, C. S., Bucknam, R. C., Blakely, R. J., Kelsey, H. M., et al. (2004). Holocene fault scarps near Tacoma, Washington, USA. *Geology*, *32*(1), 9–12. https://doi.org/10.1130/g19914.1

Sherrod, B. L., Bucknam, R. C., & Leopold, E. B. (2000). Holocene relative sea level changes along the Seattle fault at restoration point, Washington. *Quaternary Research*, *54*(3), 384–393. https://doi.org/10.1006/qres.2000.2180

Sibson, R. H. (1996). Structural permeability of fluid-driven fault-fracture meshes. *Journal of Structural Geology*, *18*(8), 1031–1042. https://doi.org/10.1016/0191-8141(96)00032-6

Skarke, A., Ruppel, C., Kodis, M., Brothers, D., & Lobecker, E. (2014). Widespread methane leakage from the sea floor on the northern US Atlantic margin. *Nature Geoscience*, *7*(9), 657–661. https://doi.org/10.1038/ngeo2232

Sultan, N., Garziglia, S., & Ruffine, L. (2016). New insights into the transport processes controlling the sulfate-methane-transition-zone near methane vents. *Scientific Reports*, *6*(1), 1–9. https://doi.org/10.1038/srep26701

Sun, T., Ellis, S., & Saffer, D. (2020). Coupled evolution of deformation, pore fluid pressure, and fluid flow in shallow subduction forearcs. *Journal of Geophysical Research: Solid Earth*, *125*(3), e2019JB019101. https://doi.org/10.1029/2019jb019101

Sutherland, D. A., Parker, M. C., Banas, N. S., & Smedstad, L. F. (2011). A model study of the Salish Sea estuarine circulation. *Journal of Physical Oceanography*, *41*(6), 1125–1143. https://doi.org/10.1175/2011jpo4540.1

Tauzin, B., Bruno, R., Perrillat, J.-P., Debayle, E., & Bodin, T. (2017). Deep crustal fracture zones control fluid escape and the seismic cycle in the Cascadia subduction zone. *Earth and Planetary Science Letters*, *460*, 1–11. https://doi.org/10.1016/j.epsl.2016.12.007

ten Brink, U., Molzer, P. C., Fisher, M. A., Blakely, R. J., Bucknam, R. C., Parsons, T., et al. (2002). Subsurface geometry and evolution of the Seattle fault zone and the Seattle basin, Washington. *Bulletin of the Seismological Society of America*, *92*(5), 1737–1753. https://doi.org/10.1785/0120010229

ten Brink, U. S., Song, J., & Bucknam, R. C. (2006). Rupture models for the AD 900–930 Seattle fault earthquake from uplifted shorelines. *Geology*, *34*(7), 585–588. https://doi.org/10.1130/g22173.1

Thomson, R. E., Mihály, S. F., & Kulikov, E. A. (2007). Estuarine versus transient flow regimes in Juan de Fuca Strait. *Journal of Geophysical Research*, *112*(C9). https://doi.org/10.1029/2006jc003925

Upstill-Goddard, R. C., Barnes, J., Frost, T., Punshon, S., & Owens, N. J. P. (2000). Methane in the southern North Sea: Low-salinity inputs, estuarine removal, and atmospheric flux. *Global Biogeochemical Cycles*, *14*(4), 1205–1217. https://doi.org/10.1029/1999gb001236

U.S. Geological Survey. (2021). *Quaternary fault and fold database of the United States*. Retrieved from https://www.usgs.gov/natural-hazards/earthquake-hazards/faults

Veloso, M., Greinert, J., Mienert, J., & De Batist, M. (2015). A new methodology for quantifying bubble flow rates in deep water using splitbeam echosounders: Examples from the Arctic offshore NW-S Svalbard. *Limnology and Oceanography: Methods*, *13*(6), 267–287. https://doi.org/10.1002/lom3.10024

Vidale, J. E., Hotovec, A. J., Ghosh, A., Creager, K. C., & Gomberg, J. (2011). Tiny intraplate earthquakes triggered by nearby episodic tremor and slip in Cascadia. *Geochemistry, Geophysics, Geosystems*, *12*(6). https://doi.org/10.1029/2011gc003559

Walker, S. L., Baker, E. T., Massoth, G. J., & Hey, R. N. (2004). Short-term variations in the distribution of hydrothermal plumes along a superfast spreading center, East Pacific Rise, 27° 30′–32° 20′ S. *Geochemistry, Geophysics, Geosystems*, *5*(12). https://doi.org/10.1029/2004gc000789

Wang, X., Niu, L., Dong, F., Hu, Y., Bayon, G., Liang, Q., et al. (2018). Using chemical compositions of sediments to constrain methane seepage dynamics: A case study from Haima cold seeps of the South China Sea. *Journal of Asian Earth Sciences*, *168*, 137–144. https://doi.org/10.1016/j.jseaes.2018.11.011

Wells, R., Bukry, D., Friedman, R., Pyle, D., Duncan, R., Haeussler, P., & Wooden, J. (2014). Geologic history of Siletzia, a large igneous province in the Oregon and Washington Coast Range: Correlation to the geomagnetic polarity time scale and implications for a long-lived Yellowstone hotspot. *Geosphere*, *10*(4), 692–719. https://doi.org/10.1130/ges01018.1

Wells, R. E., Blakely, R. J., Wech, A. G., McCrory, P. A., & Michael, A. (2017). Cascadia subduction tremor muted by crustal faults. *Geology*, *45*(6), 515–518. https://doi.org/10.1130/g38835.1

Wiesenburg, D. A., & Guinasso, N. L. (1979). Equilibrium solubilities of methane, carbon monoxide, and hydrogen in water and sea water. *Journal of Chemical & Engineering Data*, *24*, 356–360. https://doi.org/10.1021/je60083a006

Young, C., & Lupton, J. E. (1983). An ultratight fluid sampling system using cold-welded copper tubing. *Eos, Transactions American Geophysical Union*, *64*(45), 735.